Contents

Publication policy

The ECMWF Newsletter is published quarterly. Its purpose is to make users of ECMWF products, collaborators with ECMWF and the wider meteorological community aware of new developments at ECMWF and the use that can be made of ECMWF products. Most articles are prepared by staff at ECMWF, but articles are also welcome from people working elsewhere, especially those from Member States and Co-operating States. The ECMWF Newsletter is not peer-reviewed.

Editor: Bob Riddaway

Typesetting and Graphics: Rob Hine

Any queries about the content or distribution of the ECMWF Newsletter should be sent to Bob.Riddaway@ecmwf.int

Contacting ECMWF

Shinfield Park, Reading, Berkshire RG2 9AX, UK

Fax: . . . . +44 118 986 9450

Telephone: National 0118 949 9000

International . . . . . . +44 118 949 9000

ECMWF website . . . . . . http://www.ecmwf.int

EDITORIAL

Early warning of severe weather

SINCE its beginning, ECMWF has maintained a steady rate of improvement of its medium-range weather forecasts. But what is probably the most striking element in the last two years was the successful forecast, several days in advance, of most of the synoptic-scale severe weather events such as:

- The major storms that hit Europe like Kyrill in 2007 and Emma in 2008.
- The severe floods affecting the United Kingdom in July 2007 or Eastern Europe in July 2008.
- The storm-surge in the North Sea in November 2007.
- The heat wave affecting south-eastern Europe in July 2007.

It was also the case for the major tropical cyclones such as Sidr in 2007 and Nargis in 2008 in the Indian Ocean, and Gustav and Ike in the Atlantic this last September. It is important to note that these events caused extensive damage, and for some of them there were numerous casualties.

This progress is in line with the main requirement of our Member States and was set as the priority when the ECMWF strategy was discussed three years ago. Reliable forecasts of severe weather events are clearly what our modern society expects of meteorologists. The possibility of providing early warning is a significant step as it allows action to be taken in preparation for the event. Some major decisions, like an evacuation, can only be taken if sufficient time is given. This is also important in the context of climate change adaptation, as it is now recognised that the frequency and intensity of severe weather events (e.g. heat waves, storms and floods) are likely to increase. Moreover some events will become more dangerous (e.g. a storm-surge happening with higher sea level).

These successful forecasts are undoubtedly the result of the sustained improvement of the forecasting system in all areas from assimilating more data, in particular from satellites, to a complete upgrade of the physics, in particular concerning moisture and clouds, all of which are at a higher resolution. In the case of tropical cyclones, an important point was that in most cases a forecast for a given event was available several days before it was actually named. Another major contributor is the development of a probabilistic approach with specific products such as the Extreme Forecast Index.

This is certainly not the end of the story and further improvement is required. In addition specific developments are now necessary. First of all, building a reliable forecasting system means that one should not only look at successful forecasts but also at the misses and even more importantly at the false alarm. In other words we need an objective verification system for extreme events which we do not have yet. More importantly such forecasts can only be useful if properly embedded in a comprehensive warning system which includes many partners, in particular civil protection services. It will now be the task of national meteorological services to convince these partners to make use of the early warnings – this will be challenging. But this is certainly very good news as it will further increase the role and usefulness of meteorological services in our societies.

Dominique Marbouty

Changes to the operational forecasting system

DAVID RICHARDSON

Testing of new cycle (Cy33r2)

A new cycle of the ECMWF forecast and analysis system, Cy33r2 (internally labelled Cy35r1), was implemented on 30 September. The main changes in this cycle are:

- Use of OSTIA high-resolution sea surface temperature produced by the Met Office and the corresponding sea ice analysis product provided by the EUMETSAT ocean and sea ice SAF.
- Conserving interpolation scheme for trajectory fields in 4D-Var.
- New variational bias correction (VarBC) bias predictors to allow correction of infrared shortwave channels affected by solar effects (day/night variations).
- Changes to physics for melting of falling snow, albedo of permanent snow cover (e.g. over Antarctica), diurnal variation of sea surface temperature, and linear parametrization schemes.
- Convective contribution added to wind gusts in post-processing.

The physics changes will resolve the over-prediction of snow in certain marginal situations that was experienced on some occasions last winter. Otherwise changes in this cycle are mainly in preparation for future developments and there is no major meteorological impact.

ECMWF Educational Programme 2009

ELS KOOIJ-CONNALLY

ECMWF has an extensive education and training programme to assist Member States and Co-operating States in the training of scientists in numerical weather forecasting, and in making use of the ECMWF computer and archive facilities.

The courses fall into three broad categories.

- ***Use of computing facilities.*** This provides an introduction to ECMWF's computing and archive facilities. The topics covered include GRIB API, SMS/XCDP, MARS, MAGICS, METVIEW and use of supercomputing resources. The course is aimed at both current and potential users of the Centre's facilities.
- ***Use and interpretation of ECMWF products.*** This discusses the ECMWF products in operational weather forecasting available to the Member States. It is mainly aimed at forecasters or people with forecasting experience.
- ***Numerical Weather Prediction.*** This covers various aspects of research in NWP at ECMWF, including data assimilation and use of satellite data, numerical methods and adiabatic formulation of models, parametrization of diabatic processes, and predictability, diagnostics and seasonal forecasting.

Some training courses consist of modules that can be attended separately. Since these courses do not vary much from one year to another someone may decide to attend different modules in separate years.

In addition to the training courses there is a one-week seminar in early September consisting of a series of lectures dedicated to one specific topic. In 2009 the subject is '*Diagnostic Techniques to Understand and Improve Forecasting Systems*'.

A booklet describing the educational programme and methods of application is expected to be issued in November. If you do not have access to a booklet then one can be obtained by contacting Els-Kooij.Connally@ecmwf.int. Alternatively information can be accessed via the ECMWF website by going to:

- www.ecmwf.int/newsevents/training/2009

New items on the ECMWF website

ANDY BRADY

ECMWF Annual Seminar 2008

Increasingly models are being developed and used at higher resolutions. However, many physical processes remain unresolved and need to be parametrized. Even the highest resolution limited area models still need a parametrized representation of shallow convection, turbulence, microphysics, radiation and land surface processes. Schemes for deep convection and subgrid orography will still be needed in the foreseeable future for global NWP and climate models. These topics were covered at the ECMWF Annual Seminar on '*Parametrization of Subgrid Physical Processes*' which was held on 1–4 September. The presentations from the Seminar are available.

- www.ecmwf.int/newsevents/meetings/annual_seminar/2008/

Ducting Climatology

The Ducting Climatology Atlas is a five-year climatology of seasonal mean ducting frequencies of occurrence and trapping layer base heights derived from ECMWF six-hourly operational T511L60 analyses. The main motivation to create this climatology was to document how frequently the propagation of weather radar beams is likely to be affected by super-refraction or even ducting conditions over various regions of the globe. The occurrence of such situations can have serious implications for the usefulness of weather radar data in the validation of NWP outputs and also in radar data assimilation for which preliminary studies have started at ECMWF.

- www.ecmwf.int/research/physics/ducting/

Metview 3.11-export released

The latest version of ECMWF's meteorological workstation software, Metview, has been released. Version 3.11-export uses ECMWF's GRIB_API for GRIB data handling, enabling the processing of GRIB 2 data within Metview. Other enhancements are described on the Metview web pages and the updated online documentation.

- www.ecmwf.int/publications/manuals/metview/

Forecast Products Users' Meeting, June 2008

DAVID RICHARDSON

EACH year ECMWF organises a meeting of users of its medium-range and extended-range forecast products. During the meeting ECMWF presents a review of changes to its operational forecast systems over the past year and plans for future developments. Users report on their activities related to the use and verification of ECMWF products. The meeting also gives the opportunity for users to discuss their experience with and to exchange views on the use of ECMWF products, both with ECMWF and with each other. The 2008 Forecast Products Users' Meeting was held at ECMWF during 11–13 June. Around 50 forecast users participated, including representatives from National Meteorological Services and commercial users of ECMWF products.

Two major developments of the ECMWF forecasting systems were presented.

- In November 2007, a new cycle of the operational forecast model was introduced, which included significant changes to the model physics, including the convection scheme. This increased the activity in the forecasts, especially in the tropics which had previously been under-active.
- In March 2008, the 15-day VarEPS and the monthly forecast system were combined into a single unified forecasting system, providing consistent predictions from the medium range through to one month ahead. This substantially enhanced the resolution of the monthly forecast and introduced the coupled ocean into the medium-range EPS.

The performance of seasonal forecast System 3, introduced in March 2007, was presented, including demonstration of the new comprehensive verification system.

ECMWF products are used in a wide range of official duties and commercial applications. An increasing amount of data is available to forecasters either on their own internal web or via their workstation display systems. More countries are beginning to include EPS products on these systems. However, the ECMWF website is considered as a very important source of forecast information, especially for EPS, monthly and seasonal forecasts. The ECMWF web plots are now often used in the forecasters' routine duties. There is thus a continuing requirement for a reliable web production at ECMWF, including from countries investing in their own display systems.

The use of products from the EPS continues to expand and several countries reported on plans to develop their use of ensemble products in addition to those from the deterministic model. The monthly forecast is being used to advise government departments, especially on hydrological issues. Users reported increased use of the seasonal forecasts, providing outlooks to the public and responding to commercial demands.

In January 2008, the production schedule was revised so that all ECMWF products became available 10–25 minutes earlier (depending on product type). In response to user requests, additional pressure levels and vertical velocity in model co-ordinates were provided for the deterministic model. Also the set of ocean wave products was extended to include maximum wave height. On the ECMWF website, wind direction was added to the EPSgrams and a new EPSgram for ocean waves was added. Plots of ensemble mean and spread were added to the set of EPS products on the web. Current developments include the tracking of tropical cyclones that develop during the forecast and products related to extra-tropical cyclones.

Additional requests from users at this meeting included further extension of the range of parameters for the EPSgrams and extreme forecast index (EFI) as well as the extension of the EFI to longer forecast ranges. Users also expressed interest in the feasibility of developing products for additional weather parameters such as freezing level, cloud base and visibility.

More details of the meeting can be found in the presentations and summary which are available on the ECMWF website:

- www.ecmwf.int/newsevents/meetings/forecast_products_user/Presentations2008/

ECMWF Product Development

In progress

- Tracking of tropical cyclones developing during forecast
- Review of clustering
- Percentiles (EPS and model climate)
- Clickable EFI map to show EPS and climate distributions at a point
- Climate information on EPSgrams and EFI maps
- Possible extension of EFI (parameters, steps)
- Extra-tropical cyclone products
- Collaboration with Meteoalarm on heat wave indices

Requests for new products

- More parameters for EPSgrams and EFI; extension of EFI beyond day 5
- Additional weather parameters (e.g. freezing level, cloud base, visibility)
- Review options for classification of forecasts by weather types or regimes
- Coupling of Limited Area Wave model to EPS
- Soil moisture levels 1 and 2 for monthly and seasonal forecasts

Other requests

- Zoomable maps: display more detail for smaller regions on web plots
- More information on impact of model changes on weather parameters

GRAS SAF Workshop on applications of GPS radio occultation measurements

SEAN HEALY, PETER BAUER, JEAN-NOËL THÉPAUT

A WORKSHOP on the use of GPS radio occultation (GPSRO) measurements in Numerical Weather Prediction (NWP) and climate research was hosted by ECMWF from 16 to 18 June 2008. The workshop was co-funded by EUMETSAT's GRAS Satellite Application Facility (SAF) and ECMWF. The Global Navigation Satellite Systems (GNSS) Receiver for Atmospheric Sounding (GRAS) is an instrument carried on MetOp and its data has been actively assimilated at ECMWF since 20 May 2008.

The workshop focussed on applications of GPSRO measurements in operational NWP as well as reanalysis/climate studies. GPS radio occultation measurements are an important new addition to the global observing network: they are self-calibrated and they provide high vertical resolution, an all weather capability and long-term stability. Forecast impact studies at a number of operational NWP centres have demonstrated that GPSRO observations provide very useful temperature information, in particular in areas that are less well observed by other instruments such as the upper troposphere and the stratosphere. The measurements can be assimilated without bias correction and therefore have the potential to improve the bias correction of satellite radiance measurements. Recent studies have also shown that they provide useful information on the height of the planetary boundary layer. Furthermore, the long-term stability of the GPS radio occultation measurements suggests that they will have important applications in climate signal detection and model testing.

The workshop was attended by thirty scientists and was introduced by overview talks on the use of GPSRO in NWP and the work of the GRAS SAF. These were followed by invited presentations by international and ECMWF experts on the status of GPSRO missions, the assimilation of GPSRO observations, applications related to the planetary boundary layer and altimetry, and climate and reanalysis projects.

These topics were discussed further in three working groups centred on NWP, climate research and future systems. The groups produced a number of recommendations that were discussed in a plenary session on the last day, and those recommendations will form the basis of future research at ECMWF and other NWP centres. The workshop greatly benefited from the fact that GPSRO applications in NWP and climate represent a comparatively young and fast growing discipline, and this enabled almost the entire international community to attend this event at ECMWF.

An important focus of the discussions was the development of future GPSRO missions to build upon the success of the current system (CHAMP, GRACE, COSMIC, GRAS) and to avoid observation gaps in the period beyond 2010. The workshop participants therefore expressed a strong need for international support of a COSMIC follow-on concept. The participants also encouraged the formation of an International GPSRO working group, alongside the existing International TOVS (ITWG), Winds (IWWG) and Precipitation (IPWG) working groups that are endorsed by WMO. This would maintain the momentum created by the ECMWF GRAS SAF workshop.

Workshop programme, presentations and working group recommendations are available at:

- www.ecmwf.int/newsevents/meetings/workshops/2008/GPS_radio_occultation/

PREVIEW Data Targeting System (DTS)

CRISTINA PRATES, CIHAN SAHIN

ECMWF is participating in an eleven-month trial to assess the feasibility of operational adaptive control of the observing system. For this project, ECMWF has developed an interactive web-based Data Targeting System (DTS) to efficiently manage the data targeting process. This covers the process from the weather event selection to the request of additional observations based on model guidance on where such observations will be most beneficial. The DTS development has been carried out by ECMWF in partnership with the UK Met Office. The work is jointly funded by EUCOS and the European Commission as part of the PREVIEW Integrated Project of the EU 6th Framework Programme.

The real-time trial of the DTS began in February 2008. The trial is focused on improving short-range (1–3 day) forecasts of potentially high-impact or high-uncertainty weather events in Europe. The DTS is used on a daily basis by forecasters across Europe to request Sensitive Area Calculations (SACs). These predict locations where additional observations may reduce the uncertainty of potential severe weather events in subsequent forecasts. The DTS displays SAC results from ECMWF, the Met Office and Météo-France. Based on these results and on the available observational resources, the lead user of the DTS (an experienced forecaster located at the Met Office in Exeter) can then use the system to issue requests for additional observations.

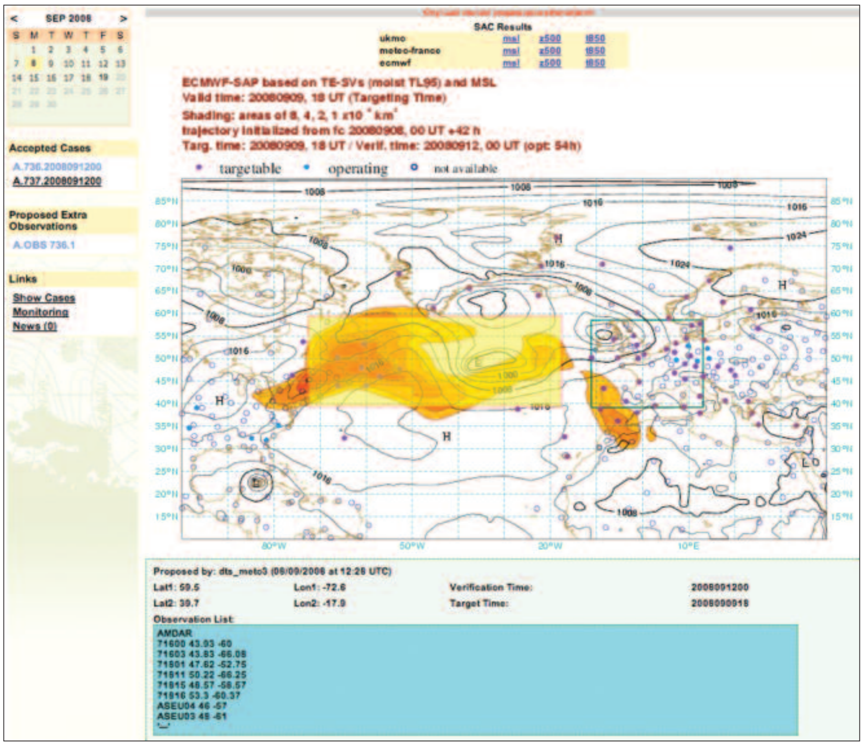

Example of a request for extra observations made by the lead user on 8 September 2008. The figure shows a snapshot of the DTS web page as seen by the lead user. In the morning of 8 September the lead user identified a case of possible severe weather on 12 September. Forecasts indicated the potential for heavy rain over western and northern France and eastern England as a sharp upper trough began to overrun a warm plume. The lead user used the DTS to mark the area that could be affected (the green rectangle) and to request sensitive area calculations (SACs) to show where additional observations on 9 September could reduce the uncertainty in later forecasts of the event. The figure shows the results from the ECMWF SACs (the shaded contours), suggesting that in this case, extra observations in eastern Canada would be most beneficial. The lead user then used the DTS to select which observations to request (in this case Canadian radiosondes, two ASAP ships and AMDAR data in the area shown in the yellow rectangle). The DTS then automatically issued requests for these observations by e-mail to the observation providers.

During the trial, observing systems that can be targeted are:

- Additional radiosonde ascents at 0600 or 1800 UTC from 64 stations managed by 17 European Met Services, Canada and Bermuda.
- Aircraft Meteorological Data Reporting (AMDAR) measurements from commercial aircraft participating in the EUMETNET observing programme.
- Radiosondes from 10 Automatic Shipboard Aerological Program (ASAP) ships operating in the Atlantic and participating in the EUMETNET observing programme.

Since the start of the trial, SACs have been requested for over 300 cases, with extra observations subsequently requested in 100 of these. To date, almost 700 additional radiosonde ascents have been requested and deployed via the DTS. An archive of the DTS usage, including a record of these extra observations, is being maintained to facilitate the future evaluation of the impact of the additional observations.

The DTS has also been used to support two THORPEX research field campaigns in 2008:

- Norwegian THORPEX-IPY experiment in the Arctic.
- T-PARC (THORPEX Pacific Asian Regional Campaign), focusing on tropical cyclones and their transition into mid-latitudes.

Later this year the DTS will also be used by the MEDEX observational experiment to study severe cyclones in the Mediterranean.

Further information about the PREVIEW project can be found at:

- www.ecmwf.int/research/EU_projects/PREVIEW/DTS/index.html

Verification of severe weather forecasts

DAVID RICHARDSON

THE ECMWF Strategy 2006–2015 puts an emphasis on early warning of severe weather and the need to develop appropriate verification. The strategy has set overall performance targets in terms of 500 hPa geopotential height for the deterministic model and 850 hPa temperature for the Ensemble Prediction System. There is a need to extend the set of headline scores that are used for long-term assessment of the performance of the ECMWF forecasting systems to include measures appropriate for severe weather. These should be based on the most important surface weather parameters and the products developed specifically to provide guidance for early warnings of severe weather, such as the extreme forecast index (EFI).

Verification for extreme weather events causes particular problems. Sample sizes are inevitably small and there are the limited time and spatial scales of the verifying observations. Also standard scores used for more moderate events may not be appropriate (e.g. they may asymptote to zero for rare events). This is a common challenge experienced in many Member States, and also an area of active research. To discuss the verification of severe weather ECMWF held a meeting with experts from Member States on 9 and 10 September.

Although at present there is no clear solution for severe weather verification, a number of possible approaches were discussed. It was noted that current verification scores for moderate events (such as are reported by ECMWF for precipitation) can give useful guidance on the expected performance for more extreme situations. Recently, new scores have been developed specifically for verification of rare events. However, there is a general lack of observations at sufficient temporal and spatial resolution for verification of severe weather. The expert team emphasised that it is essential to have such verification data and that for operational performance monitoring these need to be available in near real time. There are institutional and national datasets of high-resolution observations that would be very valuable for severe weather detection and verification.

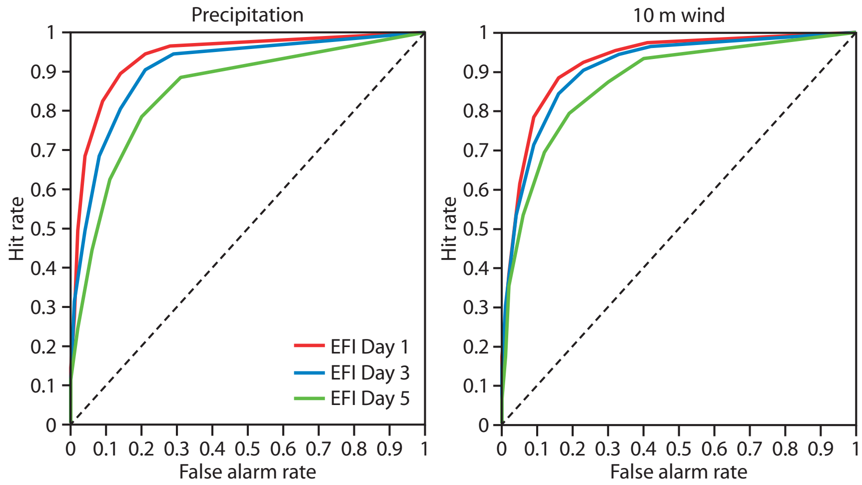

The extreme forecast index (EFI) is widely used in Member States to provide guidance to forecasters on the possible occurrence of extreme weather events. A verification procedure has been introduced to monitor the ability of the EFI to detect extreme events. The figure shows verification of Extreme Forecast Index (EFI) for precipitation (left) and 10 m wind (right) over Europe for October 2007 to March 2008 using the Relative Operating Characteristics (ROC) for probabilistic forecasts. An extreme event is taken as an observation exceeding 95th percentile of station climate. Hit rates and false alarm rates are calculated for EFI exceeding different thresholds. Results are shown for forecast days 1, 3 and 5. For both precipitation and wind the EFI demonstrates substantial ability to detect extreme events, confirming the subjective experience of forecasters.

The expert team recommended that:

- Homogeneous Europe-wide datasets are created based on institutional/national observational data (surface stations and radar data), and that these datasets be made available in near real time for the purposes of verification, particularly of heavy precipitation and strong winds. This is non-trivial and significant work is involved as data formats, quality control and reporting practices differ.
- The extreme dependency score (EDS) is explored for the purpose of extreme weather verification, together with feature-based verification and tracking of extra-tropical cyclone features.
- Estimates of uncertainty be provided for scores (whenever possible).
- Funding of verification research is promoted.

A number of areas for collaboration between ECMWF and the Member States were identified, including:

- Observation data exchange.
- Comparison of results between centres.
- Development of common scores for operational verification.
- Definition of standard sets of severe-weather test cases for Europe.

A summary of the recommendations from the meeting was presented in a discussion document to the ECMWF Technical Advisory Committee which met from 8 to 10 October.

GMES Forum, 16–17 September 2008

ADRIAN SIMMONS, BOB RIDDAWAY

FRANCE, as part of its Presidency of the European Union, and the European Commission jointly held a Forum in Lille, France, on 16 and 17 September 2008 to mark the launch of the first GMES services. The aim was to provide information about these pre-operational services and to stimulate discussion between providers and users of services. It was expected that the Forum would be of particular interest to end-users and intermediary companies providing services based on environmental information and wishing to use the results from GMES to develop new markets.

GMES (Global Monitoring for Environment and Security) offers European citizens, institutions and private companies a set of major environmental information services mainly based on Earth observations. These services will:

- Help sustainable environmental management.
- Improve understanding and knowledge to help in decision-making.
- Support the protection of people and property, especially during environment disasters, whether natural (tsunamis, earthquakes, volcanic eruptions, hurricanes, floods etc.) or man-made (marine or atmospheric pollution, deforestation etc.).

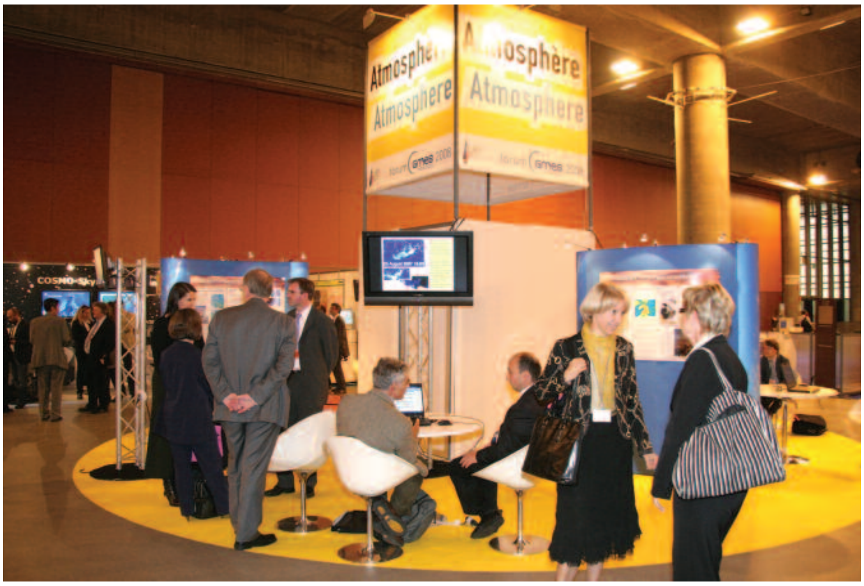

The stand dedicated to the GMES atmospheric services that formed part of the exhibition.

The Forum began with a re-branding of GMES as Kopernikus by the European Commission. The opening speeches were followed by presentations about the pre-operational services concerned with the marine environment, the atmosphere, land use and planning, crisis management after disasters, and security issues such as illegal immigration and drug trafficking. The presentation about atmospheric environmental services was given by Adrian Simmons (Coordinator for GMES Activities at ECMWF). He explained how the atmospheric services combine model simulations with world-wide observations to monitor the composition of the Earth's atmosphere and predict regional air quality using a consistent and comprehensive system. Particular attention was paid to services associated with:

- The ozone layer and UV
- "Chemical weather" and air quality
- Aerosols

Specially prepared videos on these topics were shown. They had been shot on location at DLR, Météo-France and ECMWF, respectively.

As well as the presentations and round-table discussions, there was also an exhibition which included a stand dedicated to the GMES atmospheric services. Greenhouse-gas work undertaken within these services was featured in a display on a separate stand devoted to climate. This stand included a display on reanalysis provided by ECMWF. The Centre also contributed to a smaller stand presenting the European Meteorological Infrastructure, of which ECMWF is a part.

The French Secretary of State for Transport, Dominique Bussereau, visited the stands following his closure of the meeting. He was shown some of

Adrian Simmons, Coordinator for GMES Activities at ECMWF, giving a presentation about GMES atmospheric services.

the GMES work on air quality and some of the results from ERA-Interim.

The GMES atmospheric services are currently provided by two cooperating consortia that are responsible for related projects.

- ***GEMS project***. This is funded by the European Commission, and is well advanced towards meeting its objective of putting in place integrated systems for monitoring the global distributions of atmospheric constituents important for climate, and for monitoring and forecasting constituents affecting air quality, with a focus on Europe.
  - http://gems.ecmwf.int
- ***PROMOTE GMES Service Element project***. This is funded by the European Space Agency and aims to deliver a sustainable and reliable operational service to support informed decisions on the atmospheric policy issues of stratospheric ozone depletion, surface UV exposure, air quality and climate change.
  - http://www.gse-promote.org

From mid-2009 it is expected that the core GMES atmospheric services – the central atmospheric component of Kopernikus – will be provided by a new project called MACC (Monitoring Atmospheric Composition and Climate). This will be run by an ECMWF-led consortium comprising most of the partners of the GEMS project and core production partners from PROMOTE, and funded by the European Commission under the 7th Framework Programme. It is also expected that the Framework Programme will support a set of downstream services.

Using the ECMWF reforecast dataset to calibrate EPS forecasts

RENATE HAGEDORN

WITH the unification of the ECMWF medium-range Ensemble Prediction System (EPS) and the Monthly Forecasting System on 11 March 2008 (see *ECMWF Newsletter No. 115*) a new reforecast dataset has become available for a variety of applications. A reforecast dataset is a collection of forecasts with start and prediction dates from the past, usually going back for a considerable number of years. In order to ensure consistency between reforecasts and actual forecasts, reforecasts are produced specifically with the same model system that is used to produce the actual forecasts. Before the unification of the medium-range and monthly forecast systems, reforecasts were only produced – and thus applicable – for the monthly forecast system. However, through the unification of both systems, it is now possible to use the reforecasts produced with the unified system for both the EPS and the monthly forecasts.

Originally, the reforecasts of the monthly forecast system were mainly used to determine the model climate and forecast anomalies with respect to this model climate. Now, with the reforecasts also being applicable to the medium-range EPS forecasts, new applications are possible. One of these new applications is the calibration of the medium-range EPS forecasts. Testing various calibration methods has shown that the forecasts can be significantly improved through calibration, in particular for near-surface weather parameters.

In this article we are going to discuss various questions related to calibration methods, their impact on the performance of the EPS, the added benefit of using reforecasts for calibration, and the design of the new operational reforecast dataset. Last but not least, we will make the case for ECMWF users to consider taking advantage of this new dataset, which we believe can be of enormous value for a variety of applications.

How do we apply calibration using reforecasts?

Calibration or more generally post-processing of uncalibrated Direct Model Output (DMO) is a well established technique. Many National Meteorological Services of ECMWF Member States apply this technique, also known as Model Output Statistics (MOS) or statistical adaptation, to ECMWF's DMO. A number of different calibration methods have been proposed for operational and research applications and a recent comparison of the main methods can be found in *Wilks & Hamill* (2007). Most calibration methods are based on the idea of correcting the current forecast by using past forecast errors. As such, they all require a so-called training dataset (a number of past forecast-observation pairs) to determine the optimal correction.

Until now, such post-processing activities have been mainly based on operationally available training datasets, which are either relatively short datasets or – if they cover longer times – are inconsistent datasets containing data from different model cycles or even different model resolutions. More recently it has been suggested that calibration can lead to even greater improvements if large datasets of consistent reforecasts are available and large operational weather forecast centres have been urged to provide such reforecasts (*Hamill et al.*, 2006). However, before embarking on such a reforecast programme it had to be examined whether the level of improvements, which had been demonstrated only for forecasts with relatively low quality, could also be achieved for the higher-quality ECMWF forecasts.

The reforecast dataset produced to investigate this question covers the period 1 September to 1 December, with one reforecast per week, i.e. 14 cases or start dates are available (01/09, 08/09,...,01/12). For each of these start dates, 20 reforecasts covering the years 1982–2001 are available. The reforecasts were produced with the model cycle and setup which was operational during September–December 2005 (Cy29r2, T255), except that the initial conditions were taken from ERA-40 reanalysis. Furthermore, the reforecast ensemble consists of only 15 members (1 control + 14 perturbed) instead of the operational set of 51 members. Ideally, the reforecast dataset should contain the same number of members as the real-time ensemble. However, since the production of such a full set of reforecasts seems not to be affordable in an operational setting, this option was not considered in this study – only the maximum affordable number of members were produced for this test reforecast dataset.

The first step in the calibration process is creating the training dataset. Two aspects have to be considered here: on the one hand it is desirable to have the largest possible number of training data available whilst on the other hand the training data should be as close as possible to the climate of the forecast date to be calibrated. Thus, the training dataset should be composed of reforecasts from a window centred around the date of the forecast to be calibrated. Figure 1 is a schematic showing how to compile the training dataset from the available reforecasts. The size of the window is determined by the minimal number of reforecasts needed for a reliable calibration. Window sizes of three, five, and seven weeks were tested, with five weeks turning out to be a reasonable size.

After creating the training dataset it needs to be decided which calibration method is most suitable for the specific purpose at hand. In this article we compare the results of two calibration methods:

- ***Linear Bias Correction (BC)*** – a very simple and computationally inexpensive method.
- ***Non-homogeneous Gaussian Regression (NGR)*** – a more advanced and computationally expensive method.

Whereas the BC method attempts to only correct a possible systematic shift of the ensemble mean, NGR also accounts for spread deficiencies. Further information on the calibration methods can be found in the Box A or in *Hagedorn et al.* (2008) and references therein.

What is the impact of calibrating the EPS?

The first issue to be addressed is the level of improvement that can be achieved when applying the different calibration methods. In other words, what is the impact of calibrating the EPS?

It is well known that in general the greatest impact of calibration can be seen in near-surface weather parameters since model deficiencies are most important for these (*Hamill & Whitaker*, 2007). Therefore our evaluation focuses on comparing the performance of the 2-metre temperature forecast of the uncalibrated DMO with calibrated forecasts at 250 European stations (see Figure 4 for the locations of the stations).

Box A

Calibration methods

In order to assess the different levels of improvements achievable with different calibration methods, two calibration methods have been tested.

Bias Correction

In this simplest calibration scheme, the long-term systematic error of the ensemble mean $b(x,t,l)$ is determined from the mean difference between the ensemble mean forecast $f(x,t,l)$ and the observations $o(x,t)$ in a training dataset:

$$b(x,t,l) = \frac{1}{N}\sum_{n=1}^{N} f_n(x,t,l) - o_n(x,t)$$

with: x the location, t the date of forecast, l the lead time and n the number of training cases ($n = 1,..,N$).

This long-term systematic error is then subtracted from each ensemble member of the forecast to be calibrated. Thus only the ensemble mean, but not the ensemble spread, is affected by this procedure.

Non-homogeneous Gaussian Regression

Non-homogeneous Gaussian Regression (NGR) is an extension to conventional linear regression. The basic idea is to construct a Probability Density Function (PDF) in the shape of a Gaussian, with mean and variance determined by a regression equation. The method is called "non-homogeneous" because the variance is allowed to be non-homogeneous, i.e. not the same for all values of the predictor. In this implementation of NGR, the mean forecast temperature and sample variance interpolated to the station location were predictors, and observed 2-metre temperature at station locations were the predictands. We assumed that stations had particular regional forecast biases sometimes distinct from those at nearby stations. Hence, the training did not composite the data. For example, the fitted parameters for London were determined only from London forecasts and not from a broader sample of locations around and including London.

To describe NGR more formally, let $\sim N(\alpha, \beta)$ denote that a random variable has a Gaussian distribution with mean α and variance β. Let $\overline{x}_{\text{ens}}$ denote the interpolated ensemble mean and s^2_{ens} denote the ensemble sample variance. Then NGR estimated regression coefficients a, b, c and d so as to fit:

$$N\left(a + b\overline{x}_{\text{ens}},\, c + d\, s^2_{ens}\right)$$

When $d = 0$, no spread-error relationship is in the ensemble, and the resulting distribution resembles the form of linear regression with its constant-variance assumption. The four coefficients are fitted iteratively by minimizing the Continuous Ranked Probability Score.

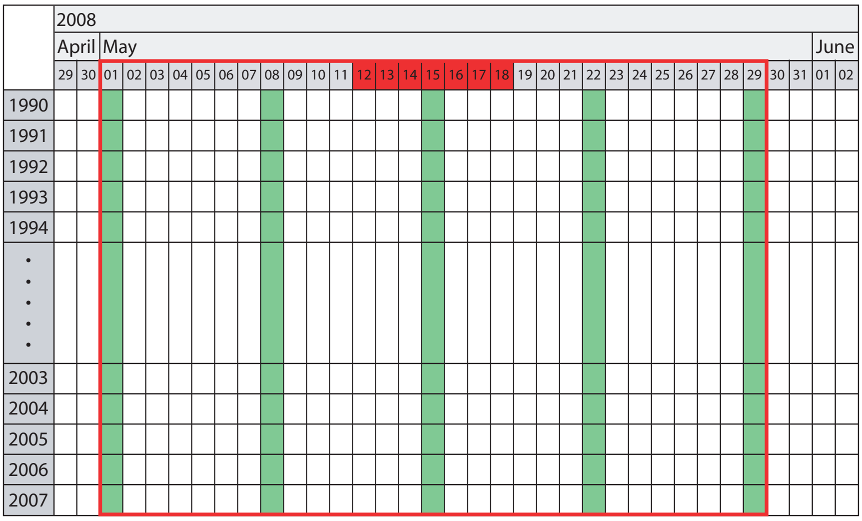

Figure 1 Schematic of available reforecast dataset and five-week window of reforecasts used as training dataset. The red frame indicates the time window used to compile the training dataset used for calibrating the forecasts started on the dates in the centre of the time window, also marked red. That is, the training dataset for calibrating the forecasts started between 12 and 18 May 2008 is composed of the reforecasts started on 1, 8, 15, 22 and 29 May, each date comprising the reforecasts from 1990–2007. The time window moves with the dates of the forecasts to be calibrated.

In order to evaluate the gridded model forecasts at irregularly spaced station location, the model forecasts were interpolated onto these stations. The main performance measure is the Continuous Ranked Probability Skill Score (CRPSS), since the CRPSS gives a good general assessment of the probabilistic forecast performance by taking into account the whole range of possible events to be forecast. A perfect forecast is assigned a skill score of 1, and a CRPSS below 0 characterizes a forecast system with less skill than the reference forecasts which here is chosen to be climatology.

Figure 2 compares the CRPSS, calculated over all 250 stations and all forecasts from 1 September to 30 November 2005, for the Direct Model Output, the Bias Corrected forecasts and the NGR calibrated forecasts. It is evident that both calibration methods significantly improve the performance of the uncalibrated model. For example, the performance of the Direct Model Output at 1-day lead time is at the same level as the performance of a 4–5 day calibrated forecast, i.e. through calibration a gain in lead time of 3–4 days can be achieved. For longer forecast lead times this gain is still around two days. When comparing the performance of the two different calibration methods it becomes clear that, particularly for early lead times, the NGR calibrated forecasts are better than purely Bias Corrected forecasts. In general, NGR can improve on Bias Corrected forecasts by two days early in the forecast range and about half a day later in the forecast range.

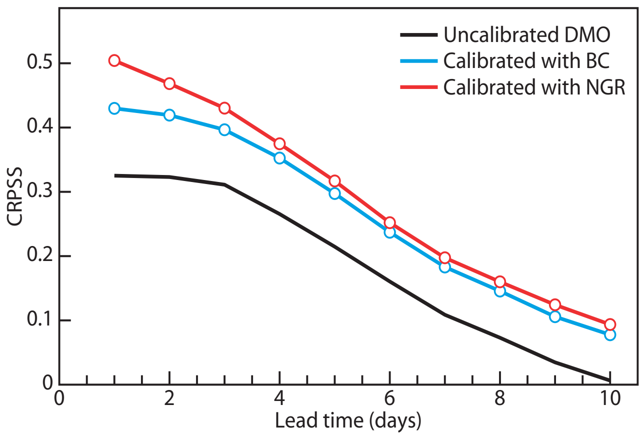

Figure 2 Continuous Ranked Probability Skill Scores of 2-metre temperature predictions at 250 European stations and for 91 cases (1 September to 30 November 2005) versus lead time. *Black line*: uncalibrated Direct Model Output. *Blue line*: calibrated predictions using the BC method. *Red line*: calibrated predictions using the NGR method.

What is the reason for the improvements in the calibrated EPS?

It is of interest to analyse the reasons for the improvements achieved by the calibration procedures. Analysing the root mean square (rms) errors and spread of the different forecasts (Figure 3) gives insight into what is happening during the calibration process. First of all, both calibration methods, BC and NGR, reduce the rms error significantly. The reduction is virtually the same for both methods, with the red and blue lines hardly being distinguishable. However, by considering

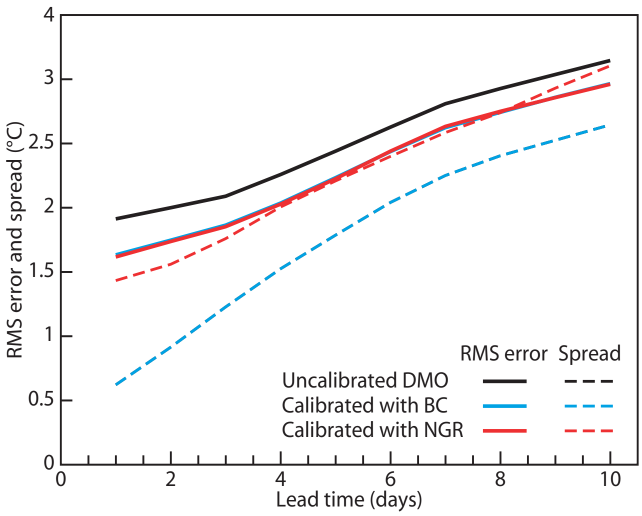

Figure 3 RMS error (solid lines) and spread (dashed lines) of 2-metre temperature predictions at 250 European stations and for 91 cases (1 September to 30 November 2005) versus lead time. *Black lines*: uncalibrated Direct Model Output. *Blue lines*: calibrated predictions using the BC method. *Red lines*: calibrated predictions using the NGR method.

additionally the changes in the spread of the forecasts it becomes clear why the NGR calibrated forecasts are improved even more compared to the Bias Corrected forecasts. It is evident that the spread of the uncalibrated DMO is much too low. Since the BC procedure does not affect the spread of the DMO, the blue and black lines are identical. In contrast, the spread of the NGR calibrated forecasts is much improved, with the spread now matching the rms error more closely. As the spread deficiency is particularly evident in the early forecast range, the NGR calibration can significantly improve the DMO over and above the BC calibration, especially at these lead times.

Figure 2 and 3 gave an overall assessment of the performance improvements for all 250 stations. However, it is also interesting to investigate the impact of the calibration at individual stations. Figure 4 gives this information by showing the CRPSS of the two-day forecasts of the Direct Model Output at individual stations (Figure 4a) and the difference in the CRPSS between NGR calibrated and uncalibrated forecasts (Figure 4b). In general, the CRPSS of the uncalibrated forecasts ranges between 0.3 and 0.7; however, there are some stations with quite low and even negative CRPSS. These stations are located mainly in areas of inhomogeneous terrain such as coastal or mountainous areas, where simple interpolation methods from gridded model forecasts to station locations are not sufficient, even when taking into account different land-sea masks etc. Obviously, at such locations calibration can be of particular value, and in fact it is the case that the differences between NGR and DMO forecasts are especially positive at these stations (Figure 4b). That is, at locations with already a fairly good performance in the uncalibrated forecasts, only moderate improvements around 0.1 can be achieved. However, in cases with particularly bad performance in the uncalibrated forecasts, calibration can achieve improvements of more than 0.2 in the CRPSS.

What is the added benefit of using the reforecast dataset?

All the calibration results shown so far were based on using reforecasts as the training dataset. However, one could certainly ask the question whether these improvements also could have been achieved by using operational forecasts from say the previous 30 days. In other words, is there really an added benefit of using a reforecast dataset?

The comparison of the performance achieved by NGR calibration using reforecasts versus the last 30 days of operational forecasts as training dataset demonstrates the level of added improvement using the reforecast dataset (Figure 5). In the early forecast range the calibration using operational forecasts as training dataset can improve the DMO nearly as much as the calibration using reforecasts. For the later forecast range, however, its performance is much worse and the calibration is no longer able to improve significantly on the uncalibrated forecasts.

So why is using the reforecast dataset particularly helpful for longer lead times? It is suggested that there are at least three contributing factors. First, the prior 30-day training data set was 9 days older for a 10-day forecast (training days −39 to −10) than for a 1-day forecast (training days −30 to −1). If errors were synoptically

a CRPSS of uncalibrated DMO

b CRPSS difference between calibrated NGR and uncalibrated DMO

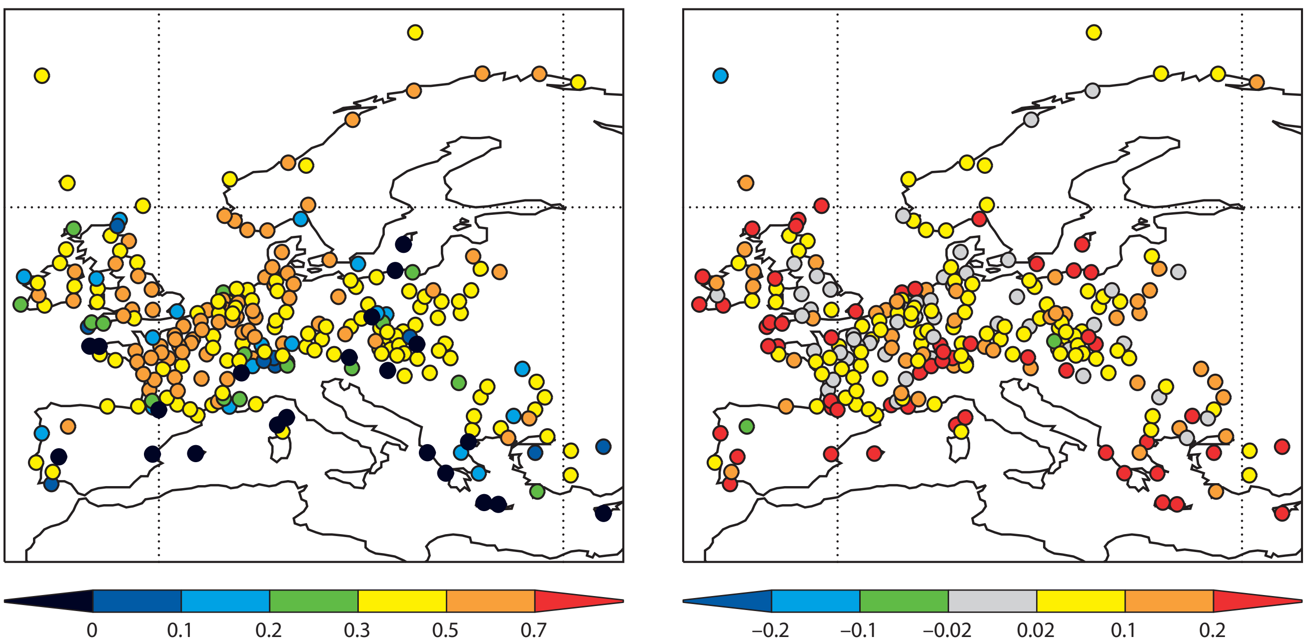

Figure 4 Continuous Ranked Probability Skill Scores of 2-metre temperature predictions at single locations, averaged over 91 cases (1 September to 30 November 2005). (a) CRPSS of uncalibrated Direct Model Output. (b) Differences between the CRPSS of the calibrated NGR and uncalibrated DMO forecasts; positive values indicate improvements by the calibration.

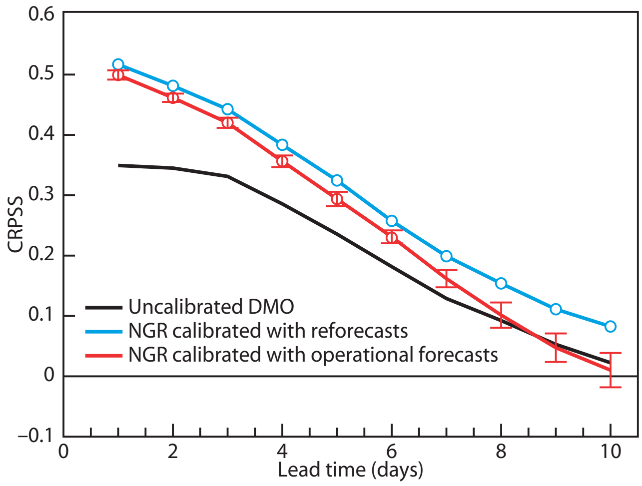

Figure 5 Continuous Ranked Probability Skill Scores of 2-metre temperature predictions at 250 European stations and for 91 cases (1 September to 30 November 2005) versus lead time. *Black line*: uncalibrated Direct Model Output. *Blue line*: NGR calibrated predictions using reforecasts as training dataset. *Red line*: NGR calibrated predictions using the last 30 days of operational forecasts as training dataset. Significance levels (0.05) of the calibration results using operational forecasts as training dataset, with respect to the calibration results using reforecasts, are denoted by the red vertical bars.

dependent and a regime change took place in the intervening 9 days, the training set at 1-day lead will include samples from the new regime while the training set at 10-days lead will not. The second reason might be due to the fact that at long leads, the proportion of the error attributable to bias shrinks due to the rapid increase of errors due to chaotic error growth. Consequently, as the overall error grows and a larger proportion is attributable to random errors, determining the bias requires a bigger sample. The third reason could be related to the fact that for the operational training data the short-lead forecasts tend to have more independent errors than the longer-lead forecasts. By contrast, the reforecast dataset, being produced only once a week, should be comprised of truly independent samples.

How is the new operational reforecast dataset designed?

Another question which had to be answered when setting up the operational production of this new reforecast dataset concerned the optimal design of this dataset, i.e. what is the best compromise in terms of costs and benefits? Decisions to be made included: "How many ensemble members are necessary and can we afford?" and "How many years should be included?" In order to answer such questions, some experiments were carried out comparing the performance of the calibration using reduced/increased reforecast datasets (Figure 6).

Increasing the number of ensemble members from 5 to 15 only adds significant benefits at longer lead times (Figure 6a). By contrast, reducing the number of available reforecast years in the training dataset from 20 to 12 reduces the performance of the calibration both in the later and earlier forecast ranges (Figure 6b). Taking into account these results, the new operational reforecast dataset comprises 5 ensemble members (1 control + 4 perturbed) and produces reforecasts for the past 18 years (currently 1990 to 2007).

First results using these operational reforecasts to calibrate most recent EPS forecasts for April to June 2008 confirm that the level of improvements actually achieved is similar to the results of the experimental calibration of the September to November 2005 forecasts. Figure 7 shows the CRPSS for the uncalibrated DMO, Bias Corrected and NGR calibrated forecasts, i.e. displays

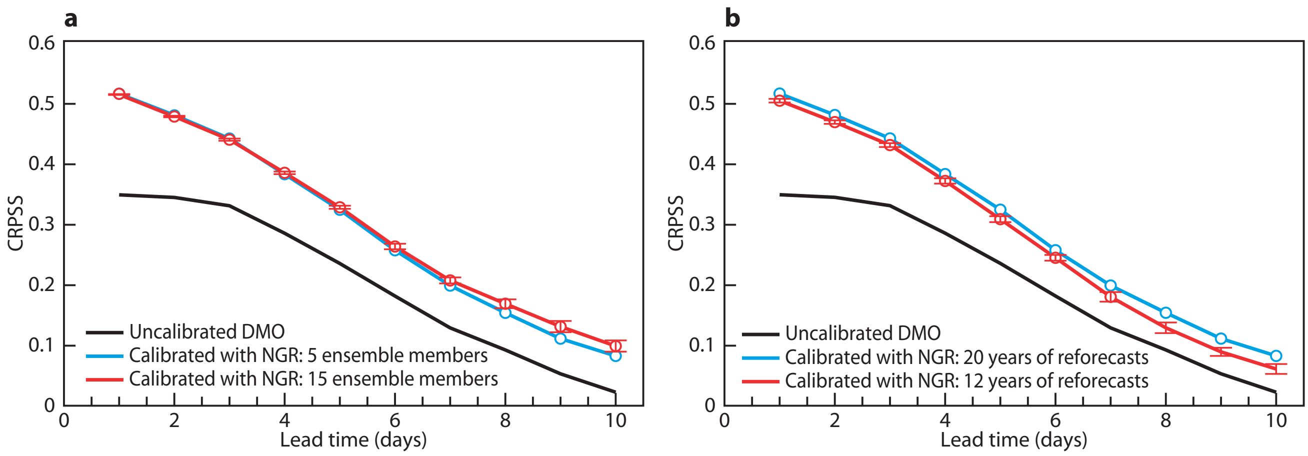

Figure 6 Continuous Ranked Probability Skill Scores of 2-metre temperature predictions at 250 European stations and for 91 cases (1 September to 30 November 2005) versus lead time. (a) Impact of increased number of ensemble members in reforecast dataset. *Black line*: uncalibrated Direct Model Output. *Blue line*: NGR calibrated predictions using only 5 enemble members of the reforecasts as training dataset. *Red line*: NGR calibrated predictions using all 15 members of the reforecasts as training dataset. Significance levels (0.05) of the calibration results using 15 members as training dataset, with respect to the calibration results using 5 members, are denoted by the red vertical bars. (b) Impact of reduced number of years. *Black line*: uncalibrated Direct Model Output. *Blue line*: NGR calibrated predictions using all 20 years of the reforecasts as training dataset. *Red line*: NGR calibrated predictions using only 12 years of the reforecasts as training dataset. Significance levels (0.05) of the calibration results using 12 years as training dataset, with respect to the calibration results using 20 years, are denoted by the red vertical bars.

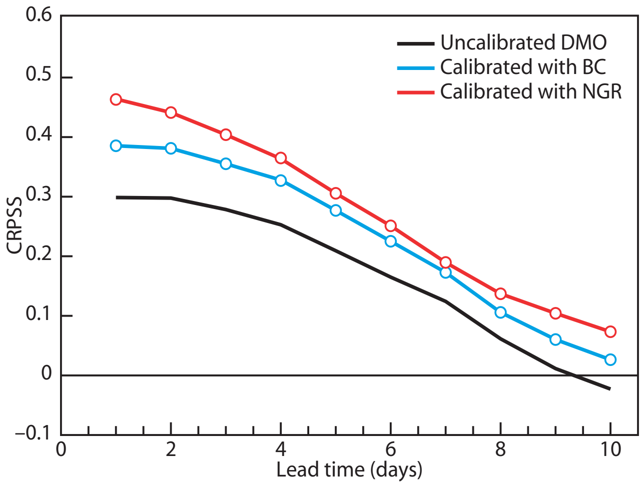

Figure 7 Continuous Ranked Probability Skill Scores of 2-metre temperature predictions at 250 European stations and for 91 cases (1 April to 30 June 2008) versus lead time. *Black line*: uncalibrated Direct Model Output. *Blue line*: calibrated predictions using the BC method. *Red line*: calibrated predictions using the NGR method. Both calibration methods use the new operational reforecasts as training dataset.

the results corresponding to Figure 1, but here for the most recent period and using the operational reforecasts as training dataset.

Who should use ECMWF's operational reforecasts?

The new set of operationally available reforecasts is opening the way to a number of applications such as site specific calibration of weather parameters, global calibration of near-surface and upper-air fields, regime dependent calibration and calibration of parameters important for specific customers. The variety of applications in itself would probably demand a variety of calibration methods, which are best developed by ECMWF Member States. Individual users will have their own requirements and observational datasets, and we encourage them to take full advantage of the new dataset for their specific purposes. However, a common set of calibrated products for the more standard applications could also be made available by ECMWF, should the users require so.

Apart from using the reforecasts for calibration purposes, there are also a number of other possible applications. For example, the reforecast dataset can be used for diagnostic studies including monitoring model performance and consistent assessment of variations in spread from year to year.

Another application is using the reforecast dataset in the context of ECMWF's activities on the Extreme Forecast Index (EFI). To determine the EFI, a reliable assessment of the model climate is necessary. Before the introduction of the operational reforecast dataset, the EFI climate was determined by running a 2-day forecast of the EPS-control every day for the last 30 years. Now the EFI is based on the model climate determined from the reforecast dataset. This has the advantage that the model climate can now be determined with a lead-time dependence for the whole forecast range and not only for the first two days of the forecast. Furthermore, the information added by having available five ensemble members instead of only the control also seems to be beneficial. These two advantages outweigh the slight disadvantage that the new operational reforecasts are produced only for the last 18 years and only once a week.

In summary, we hope that the new operational reforecast dataset will be useful not only directly for calibrating the ECMWF EPS forecasts, but also for a whole range of other possible applications.

FURTHER READING

Hagedorn, R., T.M. Hamill & J.S. Whitaker, 2008: Probabilistic forecast calibration using ECMWF and GFS ensemble forecasts. Part I: 2-metre temperature. *Mon. Wea. Rev.*, **136**, 2608–2619.

Hamill, T.M., J.S. Whitaker & S.L. Mullen, 2006: Reforecasts – An important dataset for improving weather predictions. *Bull. Am. Meteorol. Soc.*, **87**, 1–33.

Hamill, T.M. & J.S. Whitaker, 2007: Ensemble calibration of 500 hPa geopotential height and 850 hPa and 2-metre temperatures using reforecasts. *Mon. Wea. Rev.*, **135**, 3273–3280.

Wilks, D.S. & T.M. Hamill, 2007: Comparison of ensemble-MOS methods using GFS reforecasts. *Mon. Wea. Rev.*, **135**, 2379–2390.

Towards the assimilation of ground-based radar precipitation data in the ECMWF 4D-Var

PHILIPPE LOPEZ

SEVERAL forecasting centres are now able to assimilate cloud and precipitation observations in their numerical weather prediction (NWP) systems. Taking advantage of its operational assimilation of satellite microwave brightness temperatures in cloudy and rainy regions, ECMWF has started to assess the impact of assimilating hourly rainfall rates from the precipitation radar network in the USA.

Preliminary 1D+4D-Var assimilation experiments showed that this data can have a beneficial effect on analyses and forecasts. In particular, results suggest that the improvement found over the USA up to day 3 reaches Europe after a few days. It was also demonstrated that the assimilation of radar data in the absence of all other moisture-related observations can adequately constrain the moisture field over the USA, which is encouraging.

Background

Given the strong impact of precipitation on human activities and despite potential errors in radar measurements (see Box A), it is not surprising that operational networks of ground-based precipitation radars have already been installed in the USA, Canada, Europe, Japan, Australia, and more recently China. For many years now, data from about 150 S-band radars in the NEXRAD network has been combined with rain gauge measurements to produce hourly precipitation analyses over the continental USA with a delay of just a few hours. Similarly, OPERA (Operational Programme for the Exchange of Weather Radar Information), in the framework of EUMETNET, has taken up the challenge of combining ground-based radar information coming from 29 European countries (more than 150 radars currently, mostly C-band) into quasi-real-time continental-scale precipitation composites. In particular, this requires the elimination of numerous heterogeneities that are still present among European countries in terms of radar calibration, data processing and data format.

Since the late 1990s, increasing efforts have been devoted to try to assimilate the rapidly growing number of cloud and precipitation observations, mainly from satellites, in NWP systems. This is expected to improve analyses and forecasts of the atmosphere and of the hydrological cycle. So far, several operational forecasting centres (including NCEP, Met Office, Météo-France, Japan Meteorological Agency and ECMWF) have started to feed cloud and mainly precipitation observations into their three- or four-dimensional variational data assimilation systems (3D- or 4D-Var).

However, developments for an efficient assimilation of such data have been constantly hindered by the nonlinear nature of moist processes (saturation threshold, precipitation formation) as well as by the still large and poorly documented model and observation errors. Methods to alleviate some of these problems have been proposed (e.g. development of well-behaved simplified linearized physics packages) and implemented operationally.

Experimental assimilation of radar data over the USA

Taking advantage of ECMWF's operational 1D+4D-Var assimilation of space-borne SSM/I microwave brightness temperatures in cloudy and rainy regions over oceans,

Box A

Weather radars and associated errors

Weather radars are designed to provide three-dimensional information on atmospheric scatterers at high spatial and temporal resolutions. Scattering particles are typically hydrometeors, but they can also be cloud particles, aerosols, insects or birds. The size of scatterers that can be detected with a given radar mainly depends on the wavelength of the emitted pulse. For instance, S-band (8–15 cm wavelength) and C-band radars (4–8 cm) can provide information on larger hydrometeors (raindrops, snow flakes, hailstones) at horizontal ranges up to 150–200 km. Such radars are usually referred to as precipitation radars and constitute the backbone of fixed operational national networks. Smaller and hence more mobile X-band radars (2.5–4 cm) are also increasingly being used to measure precipitation for hydro-meteorological and nowcasting applications, but they are penalized by stronger attenuation and a shorter maximum range (about 80 km).

Radars with Doppler capabilities can also provide information on the radial component of the wind (isolated radar) or even on the full three-dimensional wind field (several overlapping radars). Radars equipped with dual polarization can help identify the phase of hydrometeors (rain, snow, hail) as well as their characteristics (shape, size).

In spite of the appeal of their extended and high-resolution spatial coverage, various errors can degrade the accuracy of weather radar measurements. Major sources of errors include:

- Bad radar calibration.
- Tilting and widening of beam with range.
- Non-uniform filling of beam with scatterers.
- Beam crossing the melting layer (bright band with sharp gradients of reflectivity).
- Anomalous propagation (super-refractive/ducting conditions).
- Beam blocking by large obstacles (orography) and ground clutter (echoes returned from ground itself, buildings, wind turbines etc).
- Attenuation by scatterers (decreases with wavelength).
- Echoes due to non-meteorological airborne scatterers (birds, insects etc.)
- Invalid Rayleigh approximation when hydrometeor size is not small compared to radar wavelength.
- Uncertainties in reflectivity-precipitation relationship, particle type and size distribution.
- Orographic seeder-feeder precipitation enhancement.
- Attenuation by water or dirt on radome.
- Post-processing (e.g. averaging, compositing).

A detailed discussion of precipitation radar errors can be found in *Šálek et al.* (2004). Various procedures have been developed to identify and eliminate radar pixels that are likely to be contaminated by some of these errors.

Box B

What is 1D+4D-Var assimilation?

The 1D+4D-Var method was originally developed by *Marécal & Mahfouf* (2003) and subsequently implemented in operations at ECMWF in June 2005 (*Bauer et al.*, 2006a,b) to assimilate SSM/I data in cloudy and rainy regions.

In this two-step approach summarized in the diagram, observations are first passed to a 1D-Var procedure that computes vertical profiles of temperature and moisture increments at each model grid point. ECMWF's physics yields temperature increments that are usually significantly smaller than moisture increments, so that they can be neglected. Moisture increments are then vertically integrated to create a pseudo-observation of total column water vapour (TCWV), which is eventually assimilated into the full 4D-Var system.

Both 1D-Var and 4D-Var rely on the minimization of a cost function that measures the distance of the unknown model state to a set of observations (single in 1D-Var) on one hand, and to a background model state (usually a short-range forecast) on the other hand, each of them being weighted with their respective error statistics (confidence).

In the case of ground-based radar precipitation observations, the choice was made to assimilate the decimal logarithm of ground-based radar rain rates rather than rain rates themselves. This ensures that distributions of errors are closer to Gaussian, which is a requirement for the variational analysis to be optimal.

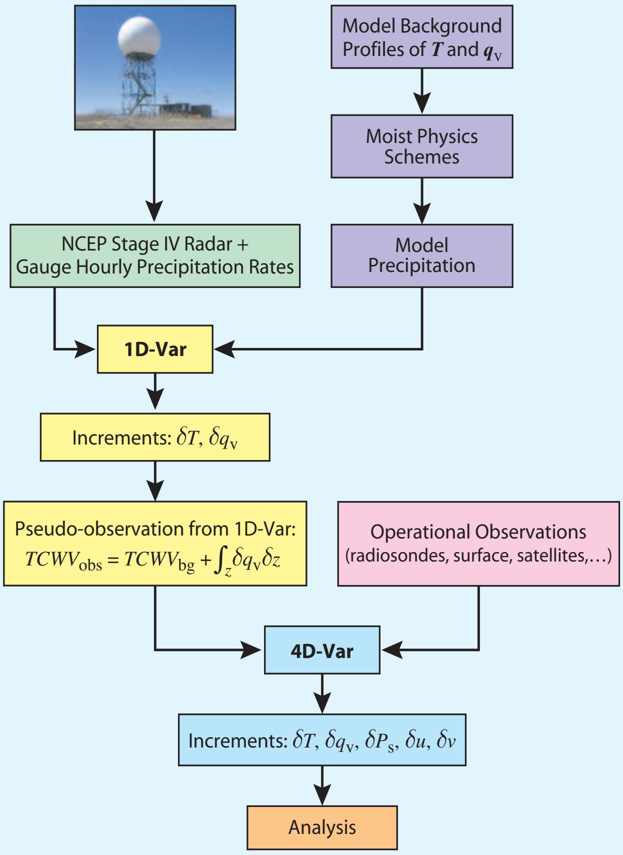

Flow chart of the 1D+4D-Var assimilation method applied to NCEP Stage IV rain rate data.

the potential benefits of assimilating rain rates from ground-based radars have been recently investigated in an experimental framework. More details on the two-step 1D+4D-Var method can be found in *Lopez & Bauer* (2007) as well as in Box B.

NCEP Stage IV hourly surface rain rate retrievals were selected because of their rather wide spatial coverage (mainland USA), their unified production and quality control processes, and their straightforward availability. This dataset combines rain rates retrieved from the NEXRAD ground-based radar network and rain gauge observations. Original 4-km resolution hourly rain rates were averaged onto ECMWF's model grid prior to assimilation. The rain observation relative error in 1D-Var was set to values between 20% over flat terrain and 50% over rugged orography. The assimilation of NCEP Stage IV rain rates was only performed at points that were rainy in both model background and observation. This led to an additional number of about 1,200 observations on average in each 4D-Var 12-hour window.

Experiments were run globally using ECMWF's 4D-Var system (cycle 29r2) at T511 spectral resolution (about 40 km) and with 60 vertical levels. Two pairs of experiments were performed from 20 May to 20 June 2005, as detailed in Table 1.

"Denial" experiments (CTRL_noqUS and NEW_noqUS) were meant to assess the actual impact of radar observations when they are assimilated in the absence of all humidity-sensitive measurements from radio-soundings, SYNOP data, and satellite infrared and microwave instruments over the USA.

Results from "full" experiments

1D-Var, which retrieves temperature and humidity information from the rain rates, was found to be well-behaved, with no need for *a priori* bias-correction. Also there was proper convergence of the iterative minimization for most points, and improved match between model and observed precipitation after 1D-Var.

As far as the final impact of the retrieved humidity information on 4D-Var analyses and forecasts is concerned, Figure 1 displays the mean NEW–CTRL differences in 4D-Var analyses of total column water vapour (TCWV) over the month of the experiments.

Experiment Type	Experiment Name	Assimilated Observations
"Full"	CTRL	All operational observations
	NEW	All operational observation + NCEP rain rates
"Denial"	CTRL_noqUS	All operational observations – all moisture observations over mainland USA
	NEW_noqUS	All operational observations – all moisture observations over mainland USA + NCEP rain rates

Table 1 Description of the precipitation radar data assimilation experiments over the USA.

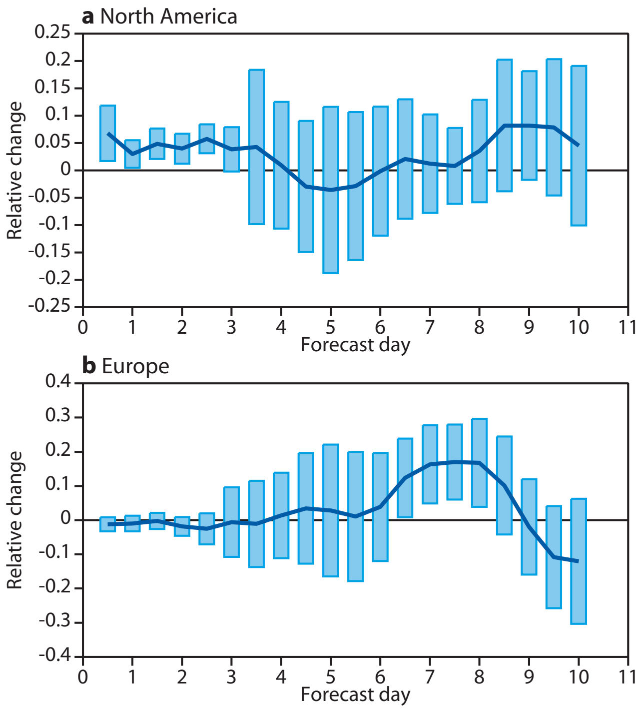

Figure 2 NEW–CTRL relative changes (unitless) in anomaly correlation of forecast 1000 hPa geopotential brought by the assimilation of NCEP Stage IV rain rates as a function of forecast range (up to 10 days) over (a) North America and (b) Europe. Positive (negative) values indicate an improvement (degradation) and blue bars show the 90% confidence level. Own verifying analyses have been used over the period 20 May to 9 June 2005.

One can see that assimilating the radar data does impact on TCWV, with well-structured patterns of drying or moistening reaching ±1.5 kg m^{-2}.

On the other hand, forecasts scores for ranges up to 10 days exhibit only insignificant changes at the scale of the northern or southern hemisphere. However, over smaller sub-domains such as North America, the North Atlantic and Europe, significant improvements can be identified when radar data is assimilated. Figure 2 displays an example of changes in anomaly correlation of 1000 hPa geopotential over North America and Europe. There is a clear improvement over North America during the first 3 days of the forecast, and over Europe around days 7 and 8. This suggests that the positive signal seen over the USA propagates downstream across the North Atlantic and over Europe. The quality of precipitation forecasts is also slightly improved but only for forecast ranges up to 24 hours.

The relatively modest overall impact of radar data on 4D-Var performance is believed to be mainly caused by the competition between the radar data and other operational observations. In particular, radiosoundings and surface station data are usually considered to be reliable and therefore are given a large weight in 4D-Var analyses.

Results from denial experiments

The purpose of the denial experiments was to investigate the potential impact of NCEP Stage IV rain rates when they are assimilated as the only source of humidity information over the USA. Figure 3 compares the mean impact on 4D-Var TCWV analyses of rejecting all operational humidity-sensitive observations from the control experiment over mainland USA [panel 3a]

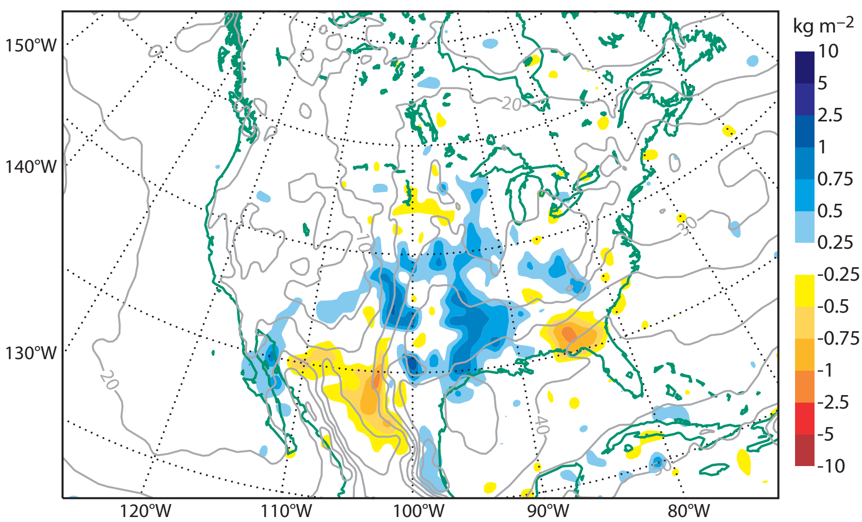

Figure 1 Mean impact of NCEP Stage IV rain rate observations on 4D-Var TCWV analyses in full experiments (NEW–CTRL). Results shown using the colour scale with positive (negative) values indicating a moistening (drying) with respect to CTRL. Isolines show the mean analysed TCWV from CTRL. Units are in kg m^{-2}.

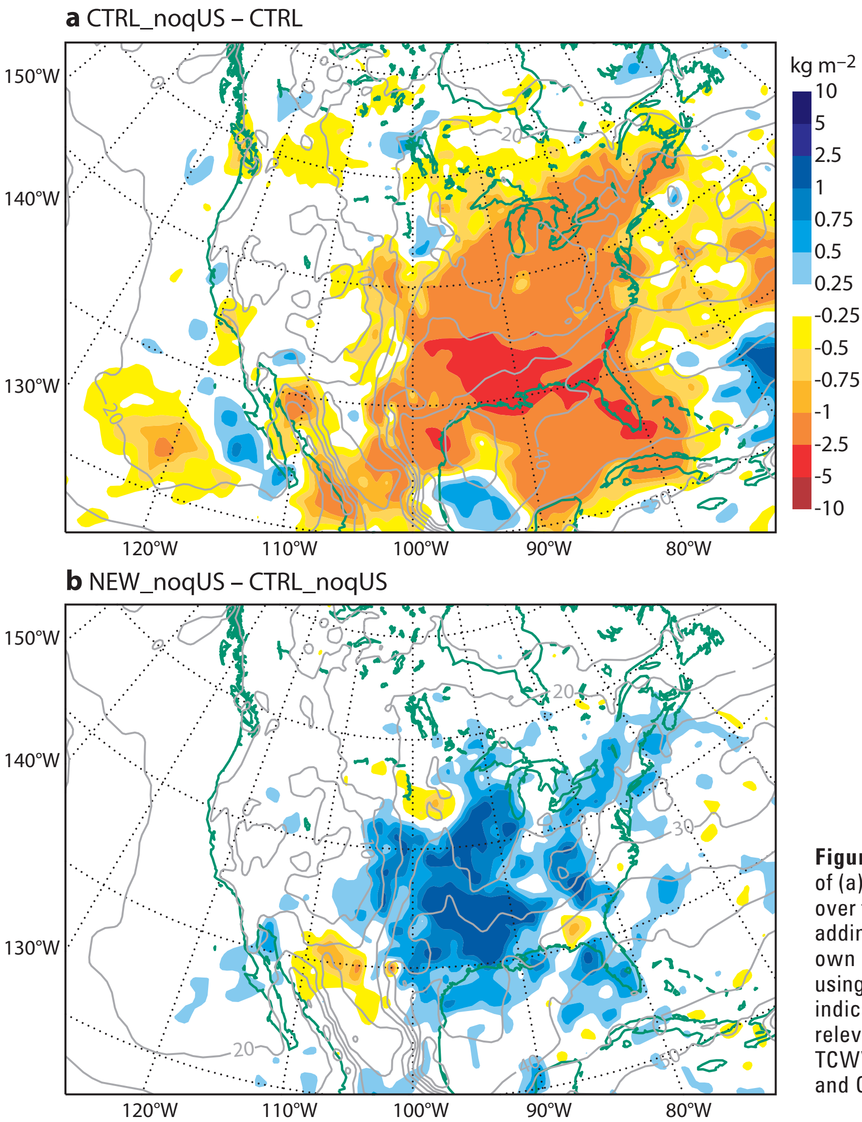

Figure 3 Mean impact on 4D-Var TCWV analyses of (a) discarding all moisture-sensitive observations over the USA in 4D-Var (CTRL_noqUS–CTRL) and (b) adding NCEP Stage IV rain rate observations on their own (NEW_noqUS–CTRL_noqUS). Results shown using the colour scale with positive (negative) values indicating a moistening (drying) with respect to the relevant control. Isolines show the mean analysed TCWV from the control experiments (CTRL for (a) and CTRL_noqUS for (b)). Units are in kg m^{-2}.

with the mean impact of assimilating the radar data alone [panel 3b]. Figure 3a shows that the lack of moisture observations leads to a substantial drying in the analyses, especially over the eastern part of the country where TCWV is usually high in springtime. On the contrary, Figure 3b clearly indicates that just adding the NCEP Stage IV rain rate data can help the analyses to recover from most of the drying seen in Figure 3a. This is encouraging and confirms that the rather small impact of radar observations found in the full experiments is due to the competition with other moisture-related observations.

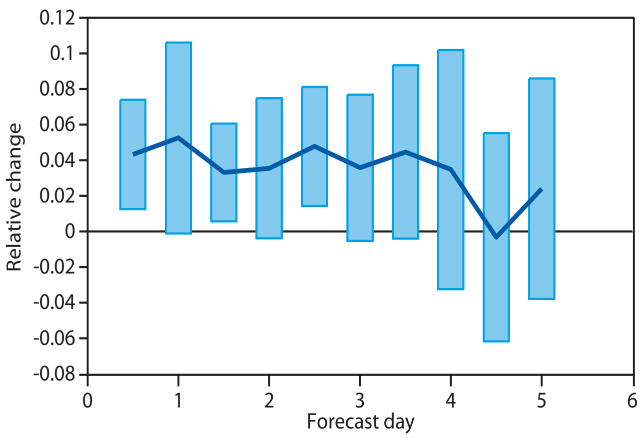

Figure 4 Relative changes (unitless) in 850 hPa temperature anomaly correlation over North America brought by the assimilation of NCEP Stage IV rain rates as a function of forecast range (up to 5 days), from "denial" experiments. Same layout and period as in Figure 2.

Furthermore, the assimilation of radar rain-rate observations in the absence of any other moisture-sensitive data over the USA significantly improves forecast scores versus own verifying analyses over this area. This is illustrated in Figure 4 that displays the relative change in 850 hPa temperature anomaly correlation, computed over 21 days over North America. The positive effect of NCEP Stage IV data on North American scores (relative improvement up to 5%) lasts for up to four days. A similar improvement is found in relative humidity and dynamical fields (not shown). Over other regions of the globe, the impact remains more neutral.

Remaining issues for cloud and precipitation assimilation

The assimilation of cloud or precipitation observations with the variational method requires efficient linearized simplified moist physical parametrizations (convection and large-scale condensation). These parametrizations, which are used in the tangent-linear and adjoint computations of the 4D-Var minimization, must be specially designed to ensure the best compromise between realism, nearness to their full nonlinear counterparts, computational efficiency and linearity. In particular, all switches associated with moist processes (e.g. saturation) must be eliminated or at least smoothed out to avoid the spurious growth of perturbations during tangent-linear and adjoint integrations.

Some questions can also be raised concerning the optimality of the indirect 1D+4D-Var approach. It is not satisfactory that this method uses the same background fields twice (first in 1D-Var, then in 4D-Var), which must result in an underestimation of the impact of precipitation observations in 4D-Var analyses. Also, the discarding of temperature increments after 1D-Var in our approach might not be suitable for all meteorological situations. In addition, feeding TCWV pseudo-observations into 4D-Var implies a loss of information about the vertical structure of the moisture field. All these reasons explain why efforts are currently dedicated to the implementation of a direct 4D-Var assimilation of rainy observations at ECMWF.

When precipitation rates or reflectivities are to be assimilated, another problem appears whenever the model background is non-rainy. In this case, the model moist physics becomes insensitive to initial conditions (mainly temperature and moisture) and the minimization of the cost function cannot be performed. Employing a first-guess which is artificially modified from the background so as to produce precipitation might alleviate this problem. This will be tested soon.

Box C

Anomalous propagation and ducting

The propagation of electromagnetic waves through the atmosphere is governed by Snell's law. In other words, it mainly depends on the spatial variations of atmospheric refractivity, N, which can be estimated using:

$$N = 0.776\ P/T + 3730\ e/T^2$$

where P is the pressure in Pascals, T the temperature in Kelvin and e is the water vapour partial pressure in Pascals. Anomalous propagation of electromagnetic waves occurs in the atmosphere for tilt angles of emission, α, lower than a few degrees and when N sharply decreases with height. It is generally assumed that when the vertical gradient of N (i.e. $\partial N/\partial z$) becomes lower than $-0.157\ \mathrm{m}^{-1}$, the wave can become trapped inside a layer (ducting) and even be deflected towards the surface. More generally, four different propagation regimes are distinguished depending on the value of $\partial N/\partial z$, as illustrated in the figure.

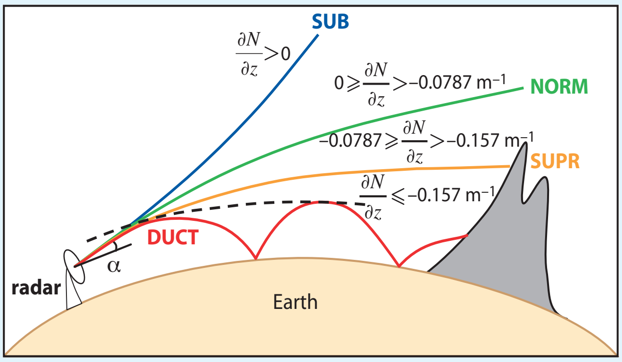

Radar beam propagation regimes according to the vertical gradient of atmospheric refractivity, $\partial N/\partial z$: SUB = sub-refractive, NORM = normal, SUPR = super-refractive, DUCT = ducting.

Meteorological situations favourable to the occurrence of anomalous propagation are characterized by an upward increase of temperature (inversion) and/or strong upward decrease of moisture, which includes:

- Temperature inversion due to nocturnal radiative cooling inside the planetary boundary layer (PBL) over land.
- Temperature inversion over a moist PBL, due to anticyclonic subsidence in the trade wind region.
- Dry air advection over sea or wet land.
- Low-level moist and cool air advection from the sea.
- Outflow of low-level moist and cold air from thunderstorms.

In the case of precipitation radars, anomalous propagation can lead to the return of spurious ground echoes and hence erroneous rainfall rate estimates.

Keeping in mind the obvious limitations associated with spatial resolution, ducting occurrence can be diagnosed from model temperature, moisture and pressure fields using the above definition of refractivity. This approach has recently led to the production of a five-year global climatology with 40-km resolution of super-refraction and ducting from ECMWF's operational analyses (*Lopez*, 2008a). This climatology might be relevant to the radar and Global Positioning System (GPS) communities but also to the broader field of telecommunications. An atlas of this climatology is now accessible to ECMWF Member States at the following address:

www.ecmwf.int/products/forecasts/d/inspect/catalog/research/physics/ducting/.

Remaining issues specific to radar assimilation

It was found that the NCEP Stage IV hourly rain rate estimates are still occasionally contaminated by anomalous propagation (see Box C) and by ground clutter, despite NCEP's quality control. For the studied period in spring 2005, such events occurred quite often over land around the Gulf of California. Figure 5 displays an example of spurious rain echoes over this region on 1 June 2005 at 2100 UTC. Most of the echoes seen on this map are due to the radar beam impinging on surrounding orography around Yuma and Phoenix, and are not associated with genuine precipitation. Feeding such data into the assimilation system might be disastrous. A stricter screening of radar data in mountainous regions should therefore be implemented in future experimentation.

Anomalous propagation events were also recently identified in OPERA data over the North Sea from a comparison to satellite precipitation retrievals, rain gauges and ECMWF short-range forecasts (*Lopez*, 2008b). Figure 6 provides an illustration of spurious radar surface rainfall estimates associated with an anticyclonic spell between 2 and 11 May 2008 over the North Sea. A procedure that diagnoses anomalous propagation and in particular ducting occurrence from model fields has been developed (see Box C). This information can help to reject dubious radar observations prior to the assimilation, as shown in Figure 6.

Also, on a few occasions, bull's-eye structures were found in the NCEP Stage IV hourly data when only rain gauge data was used to produce the rain retrieval. In the future, these undesirable patterns will be eliminated before the assimilation.

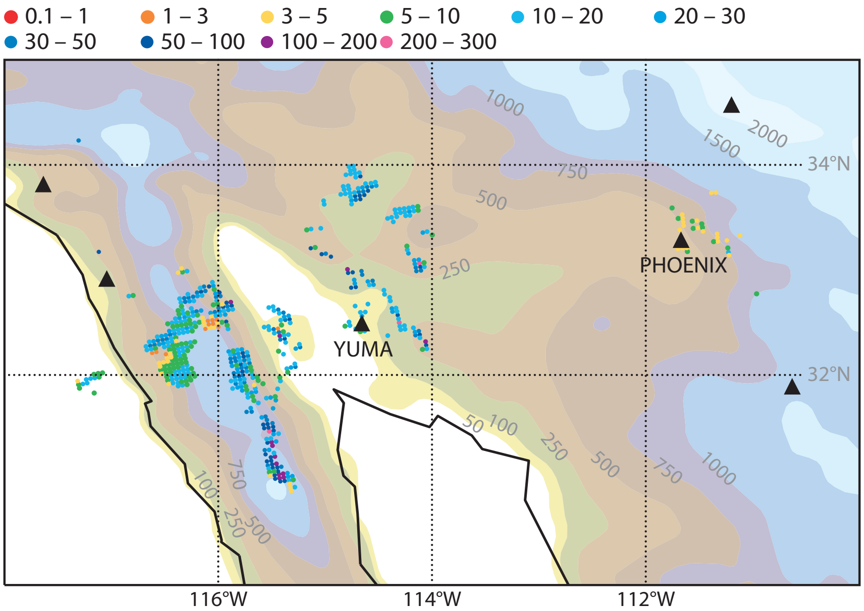

Figure 5 Example of NCEP Stage IV spurious hourly rainfall estimates over South California caused by radar beam impinging on orography (1 June 2005). Orography is colour shaded, radar rain pixels are shown as colour-coded dots and black triangles indicate radar site locations (NEXRAD network).

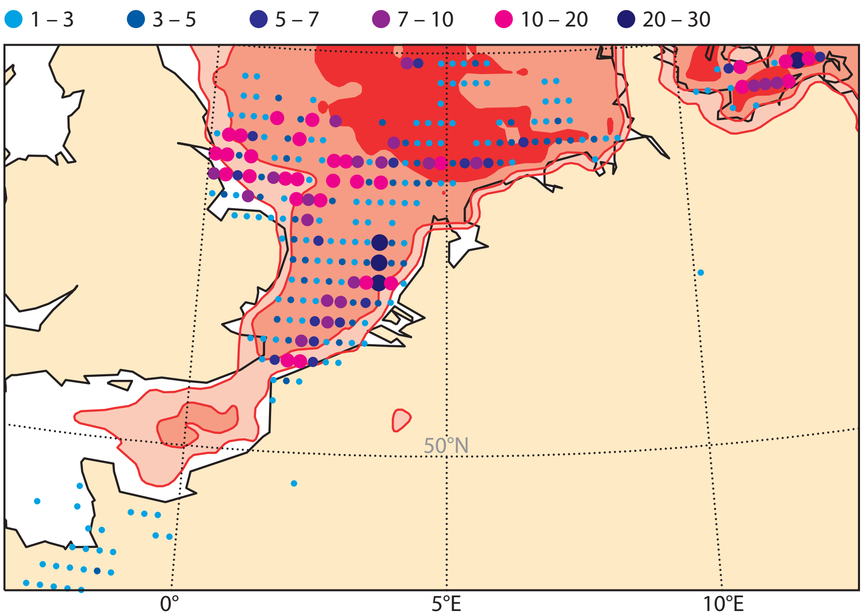

Figure 6 Spurious OPERA surface rainfall rates (dots; in mm day^{-1}) associated with anomalous propagation over the North Sea. Precipitation amounts are averaged between 2 and 11 May 2008. Frequency of ducting occurrences computed from ECMWF model analyses are shaded in red (from above 50% in pink to above 90% in red).

Over regions of steep orography, the accuracy and representativeness of ground-based radar precipitation retrievals are likely to be less than over flat terrain. Accuracy might also be an issue in snowy situations. Ideally, the question of the specification of radar observation errors should be addressed more precisely.

In addition, whether to assimilate rain retrievals or reflectivities directly is still unclear. Both methods imply underlying errors in the retrieval procedure or in the reflectivity simulator, respectively. Furthermore, neither of these approaches avoids the issue of non-rainy model background.

One should also consider whether accumulating radar data over periods of several hours could make its assimilation easier by smoothing out the effects of potential nonlinearities in the model physical parametrizations.

Eventually, a crucial prerequisite for the operational implementation of the assimilation of ground-based precipitation radar observations in the ECMWF system will be their real-time availability and exchange. This is already almost the case over the USA (NCEP Stage IV) and over Europe (OPERA).

Summary and prospects

The assimilation of NCEP Stage IV hourly rain rates over mainland USA have been tested at ECMWF in month-long global experiments, using the 1D+4D-Var technique already applied in operations to SSM/I brightness temperatures inside cloudy and rainy regions. When the radar data is assimilated in the presence of all other observations, the largest impact is found in the 4D-Var moisture analyses and for forecast ranges up to two days. Standard forecast scores (temperature, wind, geopotential) become slightly better over North America during the first three days but also over Europe on the medium-range. Precipitation forecast errors are noticeably reduced, but only within the first 24 hours. On the other hand, denial experiments without operational moisture-sensitive observations over mainland USA exhibited a large improvement in the moisture field and significantly better forecast scores over North America in the first five days when radar rain rates are assimilated. This suggests that the full benefit of the new data in 4D-Var might not be obtained in this well-observed region because of the competition with other more conventional measurements.

Ground-based radar precipitation observations have the advantage of being complementary to satellite microwave brightness temperatures that are currently assimilated over oceans only, because of strong heterogeneities in land surface emissivity. At the same time, radar data usually benefits from an excellent temporal coverage, which is not the case for microwave instruments onboard polar orbiting satellites. Furthermore, although tests performed so far at ECMWF only dealt with surface precipitation observations, one could envisage the assimilation of three-dimensional information on hydrometeors obtained from multiple radar beam elevations. The assimilation of precipitation radar data might be beneficial not only to the results of operational 4D-Var assimilation but also to those of future reanalyses as well as to soil moisture and temperature analysis.

However, several issues remain to be addressed before the operational assimilation of radar data at ECMWF becomes reality. These include:

- Selection of the best assimilation method (indirect 1D+4D-Var versus direct 4D-Var).
- Choice of the observed quantity to be assimilated (precipitation or reflectivity).
- Quantification of error statistics for radar precipitation retrievals (including the probable degradation over mountains and in snowy situations).
- Efficient rejection of dubious measurements (e.g. due to anomalous propagation or ground clutter).
- Relevance of averaging the data in time to ensure a smoother assimilation.

Eventually, the main prerequisite to the operational implementation of radar observation assimilation on a continental scale remains whether good quality data can become available in quasi real-time, at least initially over the USA and Europe.

FURTHER READING

Bauer, **P.**, **P. Lopez**, **A. Benedetti**, **D. Salmond** & **E. Moreau**, 2006a: Implementation of 1D+4D-Var assimilation of precipitation affected microwave radiances at ECMWF, Part I: 1D-Var. *Q. J. R. Meteorol. Soc.*, **132**, 2277–2306.

Bauer, **P.**, **P. Lopez**, **A. Benedetti**, **D. Salmond**, **S. Saarinen** & **M. Bonazzola**, 2006b: Implementation of 1D+4D-Var assimilation of precipitation affected microwave radiances at ECMWF, Part II: 4D-Var. *Q. J. R. Meteorol. Soc.*, **132**, 2307–2332.

Lopez, **P.** & **P. Bauer**, 2007: "1D+4D-Var" Assimilation of NCEP Stage IV Radar and gauge hourly precipitation data at ECMWF. *Mon. Wea. Rev.*, **135**, 2506–2524.

Lopez, **P.**, 2008a: A 5-year 40-km resolution global climatology of super-refraction for ground-based radar meteorology. *J. Appl. Meteorol.*, accepted.

Lopez, **P.**, 2008b: Comparison of OPERA precipitation radar composites to CMORPH, SYNOP and ECMWF model data. *ECMWF Tech. Memo. No. 569*, available from ECMWF, Reading, UK.

Marécal, **V.** & **J.-F. Mahfouf**, 2003: Experiments on 4D-Var assimilation of rainfall data using an incremental formulation. *Q. J. R. Meteorol. Soc.*, **129**, 3137–3160.

Šálek, **M.**, **J.-L. Chèze**, **J. Handwerker**, **L. Delobbe** & **R. Uijlenhoet**, 2004: Radar techniques for identifying precipitation type and estimating quantity of precipitation. *Document of COST Action 717, Task WG 1–2*, 51 pp., [available at http://www.smhi.se/cost717/doc.html], ISBN 9289800046.

The ECMWF 'Diagnostics Explorer': A web tool to aid forecast system assessment and development

MARK RODWELL, THOMAS JUNG

MANY people may be familiar with the various plots available online at ECMWF giving forecasts and forecast verification data. Here, we highlight a new set of online plots that help diagnose in more detail the performance of many aspects of the ECMWF Integrated Forecast System (IFS). These include the data assimilation system, weather forecasts and the model climate. This diagnostics package (produced by the ECMWF Diagnostics Section) is called the "Diagnostics Explorer". The present contents of the Diagnostics Explorer are summarised in Table 1. There are three main components.

- Data assimilation section includes diagnostics on observation usage and analysis increments.
- Weather forecast section includes diagnostics on forecast error and scale-dependent scores.
- Model climate section includes a wide selection of mean and variability diagnostics for both the atmospheric and coupled models.

Plots for both the data assimilation and weather forecast sections are available as seasonal means of the operational IFS (where they are compared with the same season in the previous year) and also for the tests of the experimental IFS suites (compared to the operational suite).

This article aims to introduce a representative sample of the diagnostics available in the Diagnostics Explorer and to some of the ways these diagnostics can be used. In particular, 'seamless' approaches to system diagnosis are highlighted whereby products from the data assimilation, weather forecast and model climate components can be used together to gain a better insight into the IFS. While the examples shown are of interest in their own right, they should primarily be considered as examples of how the Diagnostics Explorer can be used more generally.

IFS Component	Diagnostics
Data assimilation	***Observation space – observation usage*** • Many data sources including satellite • Data count, first-guess departures (mean, rms), bias corrections
	Model space – analysis increments • Prognostic and other parameters • Mean, standard deviation, rms • 21 pressure levels and zonal means
Weather forecast	***Forecast error*** • Prognostic and other parameters • Mean, standard deviation, rms • 21 pressure levels and zonal means
	Scale-dependent error and activity • Several parameters, levels and regions • All spatial scales and selected spatial scales
Climate of atmospheric model and coupled model	***Seasonal-means of error*** • Several diagnostics including geopotential height, winds, velocity potential, Hadley and Walker circulations, ocean waves
	Seasonal-means of variability • Blocking • ENSO teleconnections • Empirical Orthogonal Functions • Planetary and synoptic activity • Power spectra • Tropical waves (including Madden-Julian Oscillation)

Table 1 Summary of the present diagnostics available on the 'Diagnostics Explorer' website.

Assessment and interpretation of weather forecast error

Some of the most common scores used to assess weather forecast skill are based on 500 hPa geopotential heights. One example would be northern hemisphere anomaly correlations as a function of forecast lead time. A different perspective is offered by the Diagnostics Explorer.

Figure 1a shows zonal-mean root-mean-square (rms) errors in geopotential at day 5 as a function of height for the March to May season of 2005. Intelligent shading intervals are designed to cover most of the plot without being dominated by extreme values. Contours are then used, where necessary, to capture these extreme values. In the figure, the most extreme errors are found within the mid-latitude jets at around 300 hPa. Using the Diagnostics Explorer, it is possible to find out how these errors have changed over the subsequent years.

The plots in Figures 1b, 1c and 1d show the change in zonal-mean rms error in day 5 geopotential forecasts between adjacent years. Notice that statistically significant differences are indicated by bold colours (see Box A).

- ***Changes from 2005 to 2006 – Figure 1b.*** There is a reduction in errors in the southern hemisphere and above 100 hPa in the tropics, along with some degradation around 200 hPa in the tropics. While geopotential is

Box A

Statistical significance testing

To demonstrate that one model has a better mean score than another, it is essential to show that the difference in scores is large compared to the uncertainty in the estimated means. This is why statistical significance is assessed wherever possible in the Diagnostics Explorer. The assessment is made using the two-sided Student's t-test and takes account of serial correlation in the data. The significance level used is 5%. Wherever the dates for both timeseries are the same (for example in experimental-suite tests), the more powerful one-sample t-test is performed.

For the analysis increments and forecast error plots, a 'dual colour palette' has been developed to display the significant and insignificant differences. In the example in the colour bar below, a value of 3.5 would always be coloured green – a bold green is used if the value is statistically significant and a pale green is used if it is not significant. This dual colour palette draws the IFS developer's attention away from the insignificant differences that could otherwise cause unnecessary concern. Other plots use cross-hatching to indicate significance.

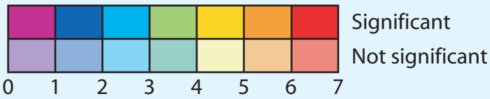

Significance testing requires access to at least 30 times more data than that stored as averages. It is not feasible to have this much data online at present and so the Diagnostics Explorer does not produce plots 'on-demand'. Instead, for every season and every experimental-suite test over 7,000 plots are produced to allow the user a lot of flexibility to explore the IFS.

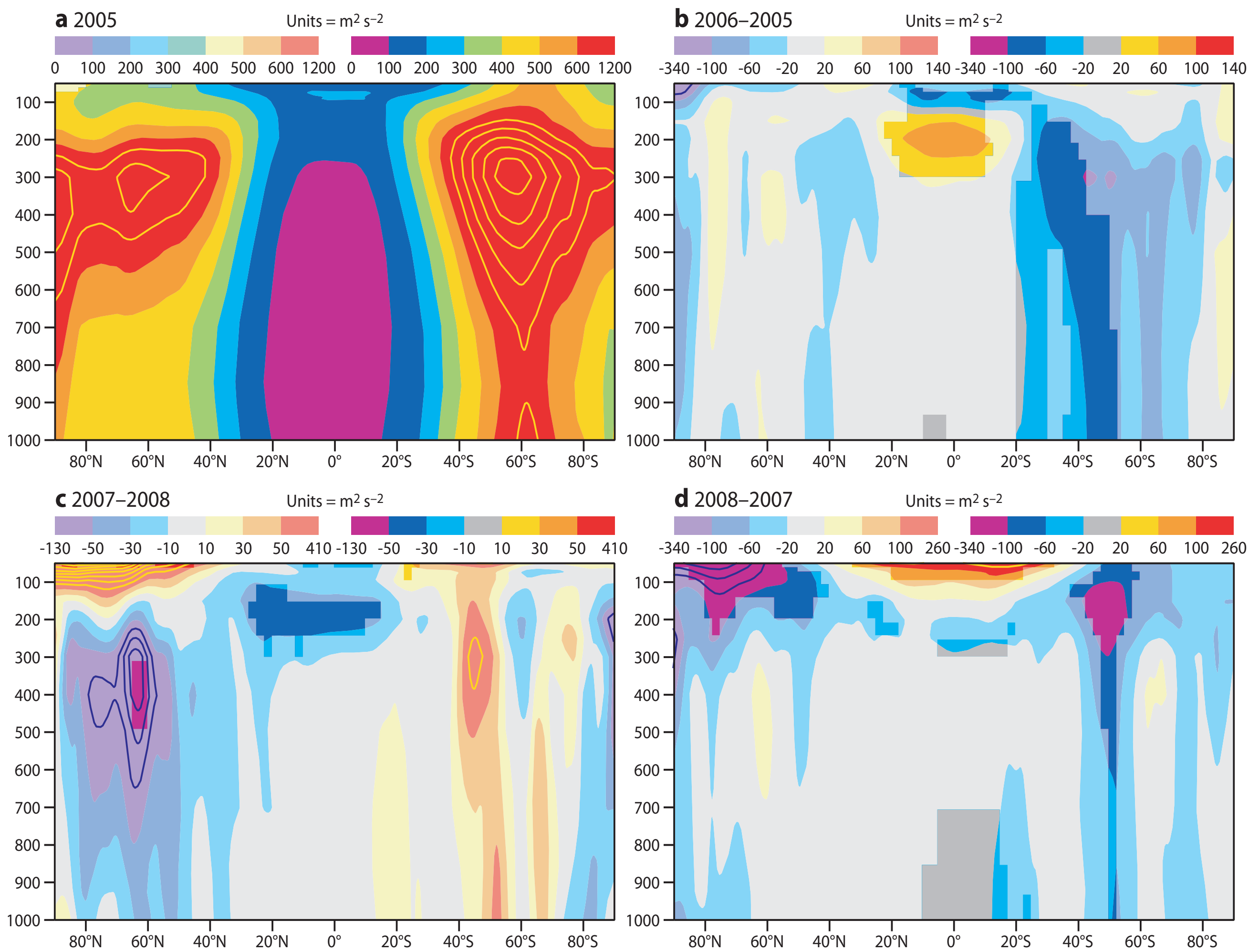

Figure 1 Zonal-mean of rms error of the five-day forecast of geopotential as a function of height for the March to May season for (a) 2005, (b) difference between 2006 and 2005, (c) difference between 2007 and 2006 and (d) difference between 2008 and 2007. Statistically significant values (at the 5% level) are shaded in bold.

not the best choice for examining the tropical atmosphere, consistent results are seen in the Diagnostics Explorer for temperature errors and these are associated with the implementation of a higher vertical resolution around the tropopause.

- ***Changes from 2006 to 2007 – Figure 1c.*** The previous tropical tropopause degradation is reversed – this improvement is associated with changes in the physical parametrization schemes including the introduction of a 'Monte Carlo' cloud over-lap scheme (*Morcrette et al.*, 2007). There are improvements in the northern hemisphere and the largest of these are statistically significant.
- ***Changes from 2007 to 2008 – Figure 1d.*** This plot is generally blue – indicating a reduction in medium-range forecast error.

Taking all the years together, it is clear that the general trend has been to reduce forecast errors.

Decreasing rms errors are generally indicative of improved skill but they can also be associated with diminishing "activity" in the model. Clearly, it is important to check for changes in activity as well as error from one model cycle to the next. In addition it is useful to know if changes in error and activity occur at planetary or synoptic scales.

Figure 2 shows forecast error (solid) and forecast activity (dotted) for planetary and synoptic scales for 500 hPa geopotential height in the northern mid-latitudes. This plot is part of the experimental suite comparison of model cycle 32r3 (Cy32r3) against the previous operational model cycle 32r2 (Cy32r2). For lead-times of 1 to 4 days, both planetary-scale error (solid, thick) and synoptic-scale error (solid, thin) are reduced in Cy32r3 (blue) compared to Cy32r2 (red). The blue circles indicate statistical significance.

Since the dotted curves indicate that Cy32r3 is more active than Cy32r2 at both spatial scales, the reduction in error must be associated with increased skill. By comparing with the observed activity in Figure 2 (dashed), the increase in synoptic-scale activity in the forecast (dotted, thin) is seen to improve the previous under-representation of activity at these scales. However, planetary-scale activity in Cy32r3 (blue, dotted, thick) grows with forecast lead-time and this over-corrects the previous under-estimation.

Forecast skill for a given spectral band is lost when the error curve (solid) meets the activity curves. It can be seen that there is still skill at synoptic scales by day 10 and even more skill at planetary scales.

The question arises as to why the planetary activity increases above the observed level in Cy32r3. A similar plot to Figure 2, but for tropical 200 hPa velocity potential, shows an earlier and more exaggerated increase in planetary activity. This suggests that tropical convection and the forcing of extratropical Rossby waves (*Rodwell & Jung*, 2008) could be involved in this change.

The activity as defined in the scale-dependent plots does not distinguish between changes in transient activity and changes in model bias. The climate runs (see Box B) provide a large amount of data and can therefore be used to distinguish between these two possibilities. Figure 3 shows power spectra as a function of longitude for tropical velocity-potential at 200 hPa from (a) ERA-40 and (b) the climate runs of the atmospheric model Cy32r3. The observations in Figure 3a show a clear peak in power at the 40–60 day timescale over the Indian Ocean and western Pacific. This is the signature of the Madden-Julian Oscillation. The atmospheric model Cy32r3 (Figure 3b) produces, for the first time, sufficient power at these timescales. However it is clear that there

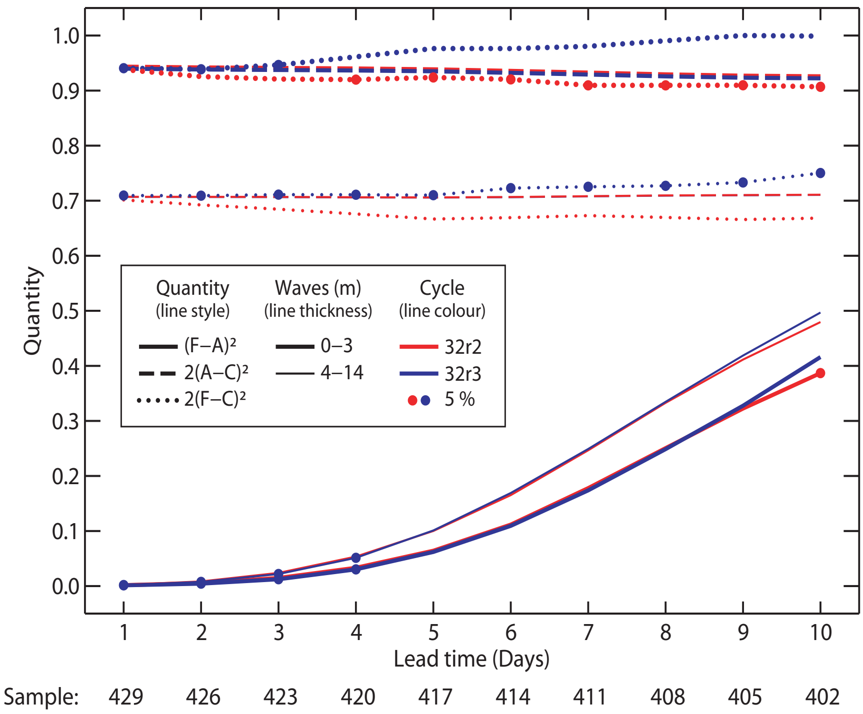

Figure 2 Mean-squared error and mean-squared activity for planetary and synoptic scale variability of the 500 hPa geopotential height in the northern mid-latitudes (35°-65°N) for Cy32r2 (red) and Cy32r3 (blue). Line style indicates the quantity. *Solid lines*: mean-squared forecast error relative to a consistent analysis [$(F-A)^2$]. *Dashed lines*: mean-squared analysis activity relative to the ERA-40 climatology [$2(A-C)^2$]. *Dotted lines*: mean-squared forecast activity relative to the ERA-40 climatology [$2(F-C)^2$]. Line thickness indicates wave-band. *Thick lines*: "planetary variability" using zonal wavenumbers 0–3. *Thin lines*: "synoptic variability" using zonal wavenumbers 4–14. Filled circles on the curve for a particular cycle indicate that the cycle is significantly better than the other cycle at the 5% statistical significance level (using a paired, two-sided t-test). All curves are normalised by the largest value on the plot. Numbers at the bottom of the figure indicate the sample size for each lead-time. The sample includes forecasts from two research experimental suites and the experimental suite run by the operations department.

Box B

Climate runs

For each model cycle, a large set of 13-month long integrations with the atmospheric component of the IFS are carried out in order to investigate the climate of the ECMWF model. Runs were started on 1 November of each of the years 1962–2005 using observed sea surface temperature and sea ice fields as lower boundary conditions. The first model cycle in the climate section of the Diagnostics Explorer is Cy29r2. The runs are carried out using a horizontal resolution of T159 with 91 levels in the vertical (60 levels prior to Cy31r1). The results are diagnosed for the four standard seasons December to February, March to May, June to August and September to November; the first month being discarded to allow the model to spin-up.

The model integrations are compared with observational data from various sources including (re-)analysis, satellite and SYNOP data. The satellite data sets have been compiled and kindly made available by scientists of the Physical Aspects Section.

is too much power at very long time scales associated with planetary waves. On the other hand, the fact that the IFS also has biases in the tropics is apparent from Figure 4 that shows systematic precipitation errors for Cy32r3.

Representation of the Indian summer monsoon

The precipitation bias of Cy32r3 can be seen in Figure 4 to extend over the Indian Peninsular. This represents an excessively strong Indian summer monsoon. A realistic representation of the Indian summer monsoon by numerical models is crucial given the large number of people directly affected by it and its potential for affecting the climate in distant locations. In addition to the excessive rainfall in Cy32r3, the low-level monsoonal winds over the Arabian Sea are also too strong. *Rodwell & Hoskins* (1996) show that these two features are intimately related but it is difficult to determine from the climate runs what comes first: the excessive rainfall or the excessive monsoon inflow. In order to shed more light on the possible origin of this error it is helpful to determine how early the strong monsoon inflow develops within the forecast.

Figure 5 shows mean 850 hPa horizontal wind errors at day 5 from the medium-range weather forecasts for (a) Cy32r3 and (b) the then operational cycle Cy32r2 for the period 11 June to 1 August 2007. Both cycles have winds that are too strong over the Arabian Sea but Cy32r3 has the strongest winds (another plot in the Diagnostics Explorer shows that this difference is statistically significant with a large magnitude of around 3 ms^{-1}). It is clear that the particularly excessive monsoon inflow in Cy32r3 starts to occur even in the medium-range.

The difference in the mean analysis increments for winds at 850 hPa between Cy32r3 (experimental suite) and Cy32r2 (operational suite) is shown in Figure 6 using data from 1 June to 1 August 2007. It can be seen that for Cy32r3 the observations have a bigger impact than in Cy32r2 in slowing down the excessive strong low-level jet produced by the first guess. Such an early appearance of the increased mean wind error strongly indicates that the cause is local to the Arabian Sea (and not caused by excessive monsoonal precipitation).

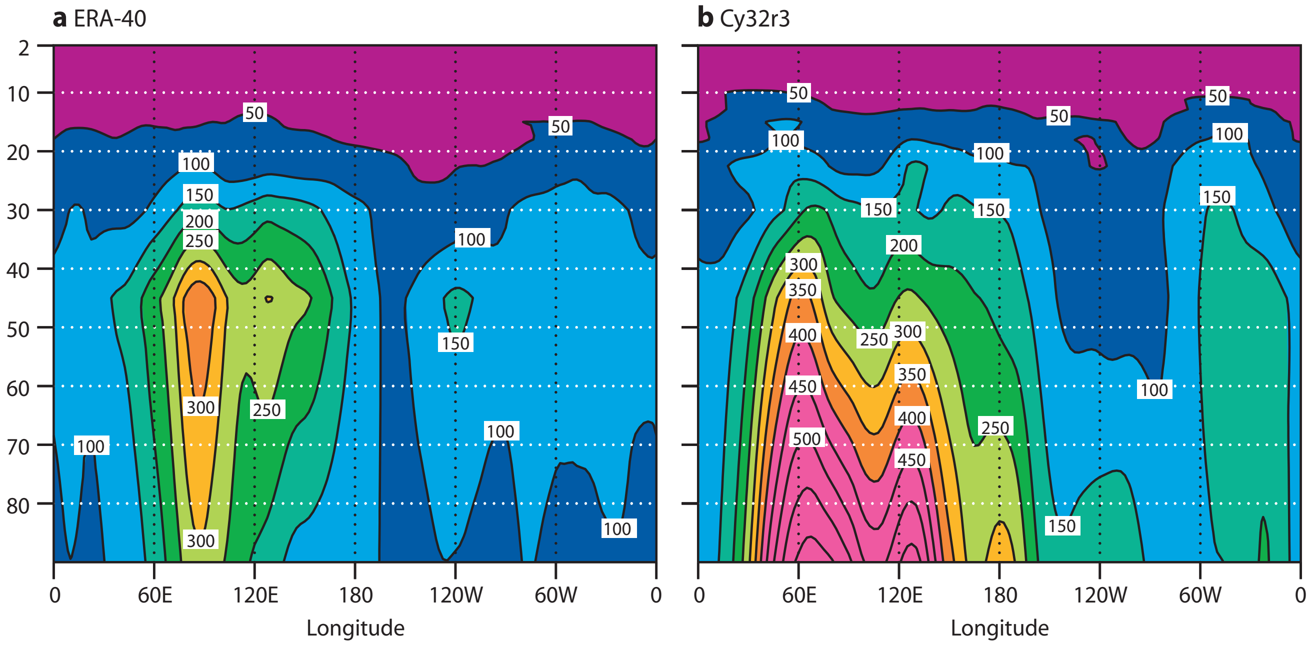

Figure 3 Average power spectra of tropical (5°S–5°N) velocity potential anomalies at 200 hPa (m^2s^{-1}) as a function of longitude for (a) ERA-40 and (b) Cy32r3. Results are based on all December–February seasons for 1962–2005. Anomalies have been computed by removing the mean annual cycle.

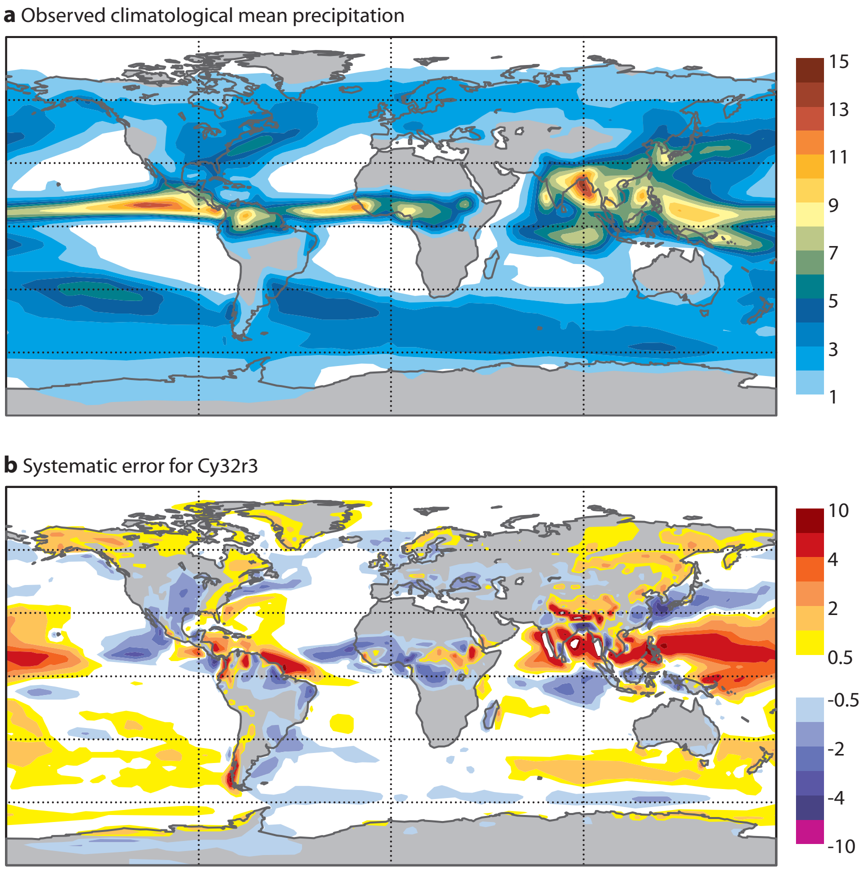

Figure 4 (a) Observed climatological mean precipitation (mm day^{-1}) from GPCP data for the June-August season for 1979–2001 along with (b) the corresponding systematic errors for Cy32r3 for 1963-2005.

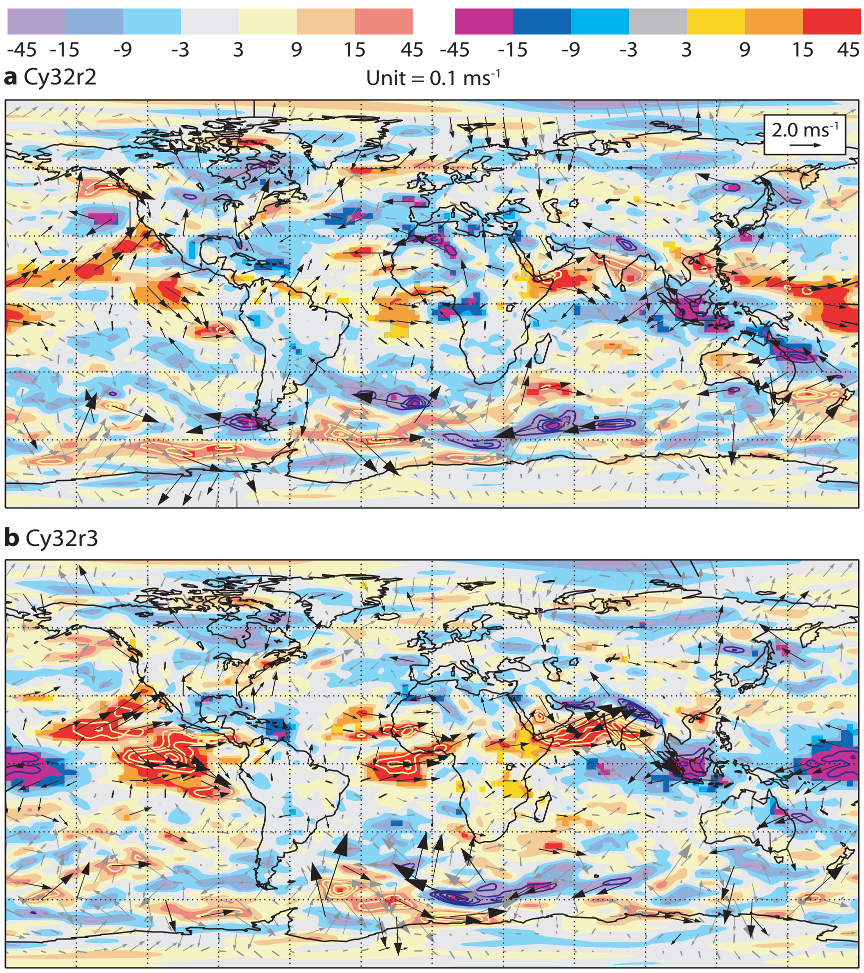

Figure 5 Mean systematic errors of the zonal wind component (shading) and horizontal winds (arrows) at 850 hPa for day 5 forecasts with (a) Cy32r2 and (b) Cy32r3. Results are based on all 00 UTC forecasts starting between 11 June and 1 August 2007.

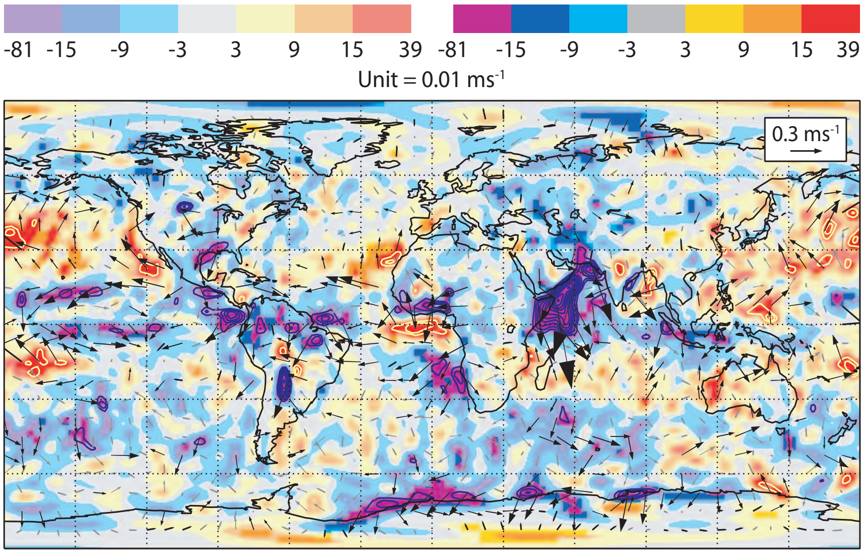

Figure 6 Change in mean analysis increments for the meridional wind component (shading) and horizontal winds (arrows) at 850 hPa from Cy32r2 to Cy32r3. Results are based on all 00 UTC and 12 UTC analyses made between 1 June and 1 August 2007.

A more detailed investigation of the analysis increments suggests that it is particularly at the lowest-most levels, where the moisture transport peaks, that the first guess produces too strong winds. Our analysis therefore suggests that the excessively strong Indian summer monsoon in Cy32r3 has its origin in problems with simulating the vertical structure of the low-level monsoonal inflow over the Arabian Sea. This could be associated with the (otherwise beneficial) change in vertical diffusion parametrization at Cy32r3. Changes to the vertical diffusion and convection scheme made in Cy33r1 have led to a moderate reduction of the overly active Indian summer monsoon.

Understanding the errors in the Hadley Circulation

The investigation of the Indian summer monsoon clearly highlights the power of a seamless approach to weather and climate – a feature that is central to the philosophy of the Diagnostics Explorer. We now consider how the data assimilation component of the Diagnostics Explorer (observation usage and analysis increments) can be used to provide a better understanding of the mean errors in the Hadley Circulation.

As an example, Figure 7a shows the zonal-mean day 2 errors in temperature and meridional circulation averaged over December to February (DJF) 2007/8. The dominant branch of the Hadley Circulation (in the northern hemisphere in DJF) is consistently forecast to be too weak. This has been a long-standing issue for the IFS. In addition, there is a temperature error in the tropics with the lower-troposphere too cool, the mid-troposphere too warm and the upper-troposphere/lower-stratosphere too cool. The analysis increments (Figure 7b) show that these temperature and meridional circulation discrepancies exist very early in the forecast. This indicates that the problem has a local (tropical) explanation. Figure 7c shows the analysis increments at 500 hPa. The cooling increment at this level can be seen to occur over much of the tropics, particularly over the Indian Ocean/western Pacific region.

Mean analysis increments show where the observations are consistently different from the model's first guess. However, they do not tell us whether it is the model or the observations that are (most) at fault.

The Diagnostics Explorer contains a section on observation usage within the data assimilation system. These plots are in "observation space" so, for example, satellite brightness temperature observations are compared with brightness temperatures simulated by the model. A brightness temperature does not reflect a temperature at a single height in the atmosphere but rather a weighted integral of temperature over an atmospheric layer. The 'AIRS' Satellite channel 215 "sees" temperatures within the 700–300 hPa layer with a maximum weighting at around 500 hPa. Figure 7d shows "first-guess departures" (observation minus first guess) for this channel. Comparison with Figure 7c shows that these departures strongly support the tropical cooling increments at 500 hPa. The magnitude of the first-guess departure can be as large as 0.9 K and generally has a value of around 0.1 K.

Having identified one set of observations that support the systematic analysis increments, it is now important to quantify the magnitude of the likely residual bias in these observations (i.e. the bias after the observation has been bias-corrected). Figure 7e shows the variational bias correction (*McNally et al.*, 2006) applied to this data by the data assimilation system. The magnitude of this correction is typically of order 0.05 K. If these corrections do account for most of the observation bias then one could conclude that residual observation bias is even smaller and not responsible for the mean analysis increment. This would then highlight model error as the more likely cause for the cooling increment. A word of caution is appropriate, however, since Figure 7f shows that the number of AIRS channel 215 observations used within the data assimilation system is generally smaller in the regions of larger mean first-guess departures. This drop in observation usage is associated with cloud screening of infrared data. The "model error"

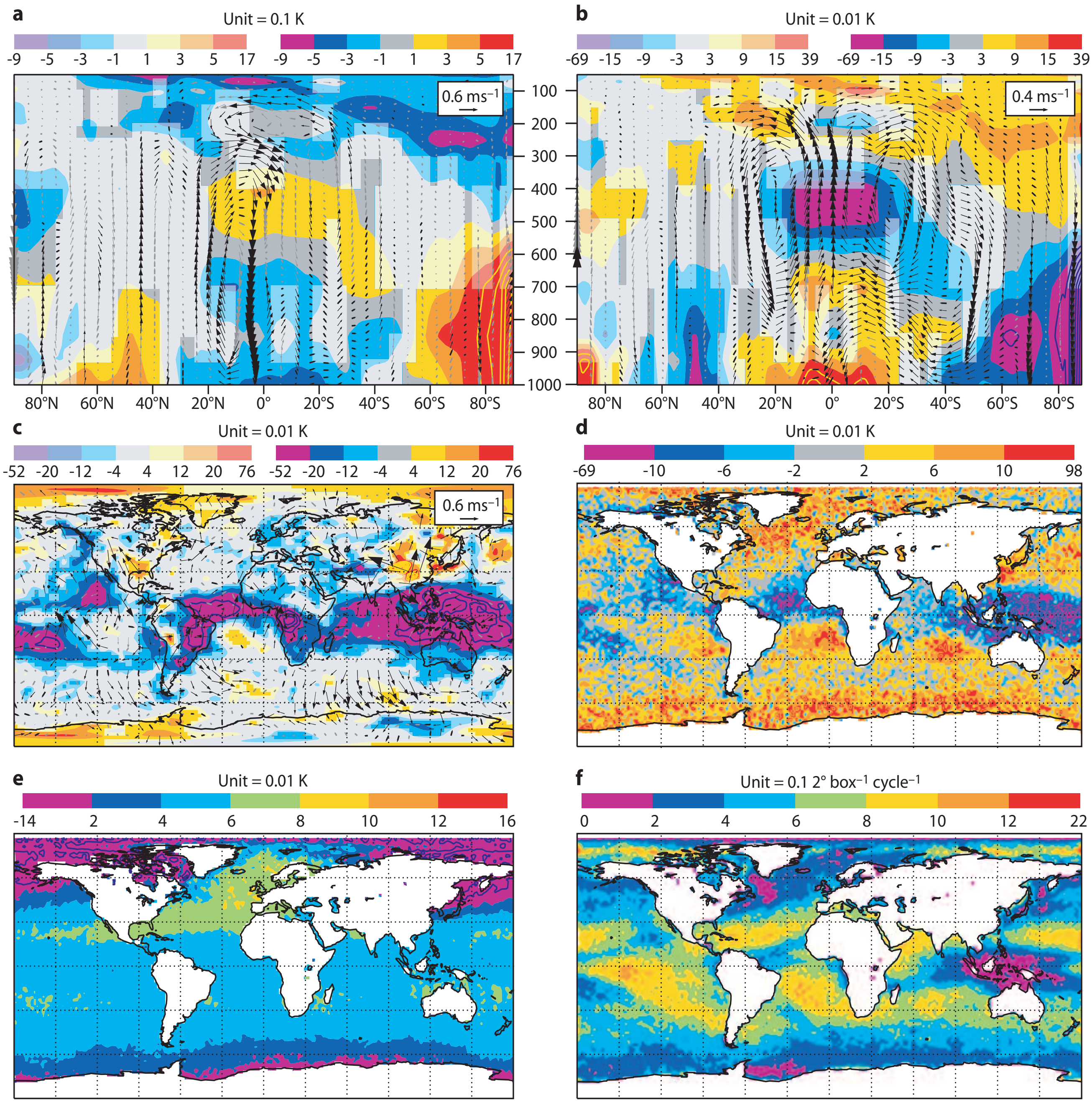

Figure 7 Results highlighting the nature of Hadley Circulation systematic error during December to February 2007/08. (a) Zonal-mean Day 2 forecast error of temperature (shaded) and meridional circulation. (b) Zonal-mean analysis increment of temperature and meridional circulation. (c) 500 hPa analysis increment of temperature and horizontal wind. (d) First-guess departures (observation minus first guess) from AIRS satellite channel 215 infrared brightness temperature. (e) Variational bias correction applied to the AIRS channel 215 brightness temperature within the data assimilation system. (f) Average number of AIRS channel 215 observations used per 2° grid-box in each data assimilation cycle.

conclusion would be stronger if other observations could be found to back-up the analysis increments. One such set of observations are the 'AMSUA' channel 5 microwave brightness temperatures. These observations can "see through" the tropical clouds and the observation count plots show that the AMSUA data are actually used more than the AIRS within the data assimilation. With the additional support of a few radiosonde stations, the "model error" conclusion appears to be quite robust.

Diagnosis of seasonal forecast bias

ECMWF runs a coupled atmosphere-ocean model to make predictions several months in advance. In the current system, called System 3 (*Anderson et al.*, 2007), the atmospheric component (based on Cy31r1 at T159L62) is coupled to the Hamburg Ocean Primitive Equation Model (HOPE). A large set of hindcasts were carried out with System 3 to allow post-processing (bias correction) of operational forecasts. Moreover, diagnostic runs (hindcasts) were carried out by members of the ECMWF Seasonal Forecast Group; for these the atmospheric component of System 3 is run in uncoupled mode by prescribing observed sea-surface temperature and sea ice fields. It can be argued that these diagnostic runs provide an estimate of the upper limit of seasonal predictability with the current system and give the opportunity to investigate the impact that atmosphere-ocean coupling has on systematic model errors.

Hindcasts with the coupled and uncoupled version of System 3 have been diagnosed and the results are available on the Diagnostics Explorer. To give an example of what can be learnt from these results, Figure 8a shows systematic error in 500 hPa geopotential height for the coupled atmosphere-ocean model. Evidently, systematic errors are quite substantial taking values of similar magnitude to those of the observed seasonal mean anomalies that System 3 aims to predict. In the North Atlantic region a cyclonic bias stands out, which is associated with an underestimation of the observed frequency of Euro-Atlantic blocking events (*Jung*, 2005). Also an anticyclonic bias is prominent in the North Pacific region. One might speculate that these errors are due to a drift of the coupled system, particularly in the tropics, which could lead to the erroneous generation of stationary Rossby waves over the northern hemisphere. The fact that the run with prescribed sea-surface temperature anomalies (Figure 8b) produces similar biases, however, suggests that the origin of this error lies in the atmospheric component of System 3. By looking at similar diagnostics for more recent model cycles, the Diagnostics Explorer reveals that recent model changes led to substantial reductions in the size of systematic errors in 500 hPa geopotential height over the North Pacific and North Atlantic.

ECMWF training courses

One of the duties of ECMWF is to assist its Member States and Co-operating States in the training of forecasters and scientists in numerical weather forecasting through an extensive educational programme. In spring 2008 the Diagnostics Explorer was used for the first time in the Predictability, Diagnostics and Seasonal Forecasting module of the NWP Course to introduce diagnostics techniques and to discuss the performance of the ECMWF forecasting system at time scales of hours (analysis), days (numerical weather forecasting) and several months (seasonal forecasting). After an introduction to the Diagnostics Explorer, the students were asked to use it to answer a set of questions. In this way the students learnt, amongst other things, about aspects of the nature of forecast error and its growth, how to assess year-to-year changes in forecast error and how to diagnose a complex data assimilation system. Given positive feedback from the students, it was decided that use of the Diagnostics Explorer will be an integral part of future training courses.

Outlook

Recently, work on the Diagnostics Explorer has focused on the development of the diagnostics software (with technical help from the Metview Team) and uploading the plots to the web (with the help of Claude Gibert from the Meteorological Operations Section). Results are now available for all components of the IFS: the data assimilation system, the wave model, the forecast model and the coupled atmosphere-ocean model. What are the plans for future developments of the Diagnostics Explorer?

The incorporation of new diagnostics, aimed at helping to understand the origin of forecast error on time scales from hours to many months, is an ongoing activity. For example, diagnostics of the vorticity balance in the atmospheric model (*Rodwell & Jung*, 2008), including the Rossby wave source, will soon be added. Furthermore, it is planned to include the results of

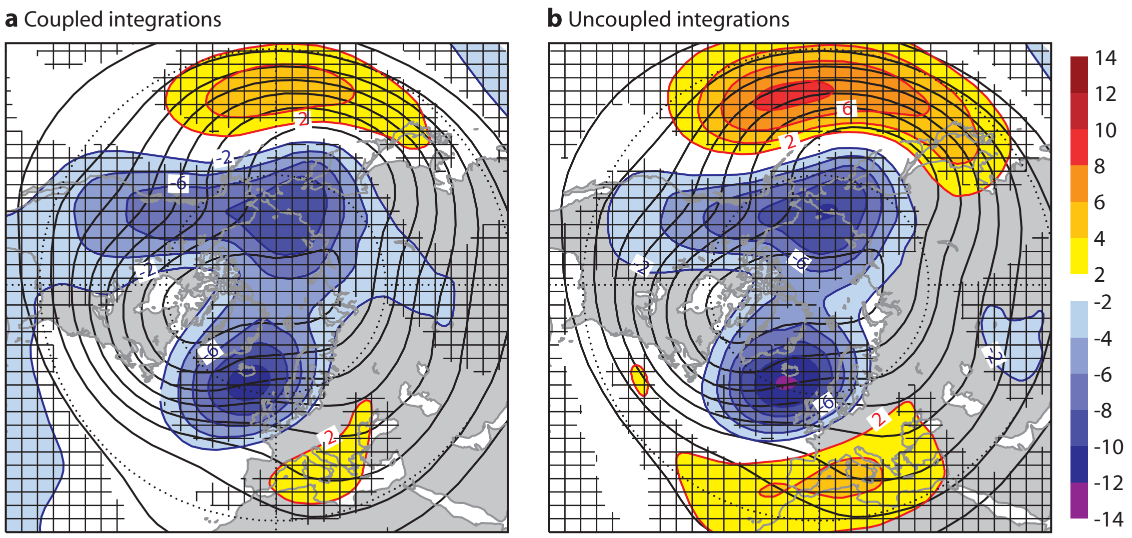

Figure 8 Mean systematic error of 500 hPa geopotential height fields (shading in dam) for December to February in 1982–2005 for (a) coupled and (b) uncoupled integrations of System 3. Statistics for the models are based on five ensemble members. Also shown are climatological mean fields from ERA-40 (contours). Mean errors that are significantly different from zero at the 5% level are hatched.

special experiments designed to address issues of particular concern. For example, model climate sensitivity to increasing resolution. With the introduction of Seasonal Forecast System 4, it is also planned to incorporate diagnostics of the ocean data assimilation system in a fashion similar to the one already used for the atmosphere. Finally, it is planned to extend the use of Diagnostics Explorer by making the software available to all scientists at ECMWF.

We hope that, with the Diagnostics Explorer and its further developments, the Diagnostics Section can make a contribution to future improvements of all components of the IFS.

Online access to the Diagnostic Explorer by Member States will be considered in the near future, subject to interest and resources.

FURTHER READING

Anderson, **D.**, **T. Stockdale**, **M. Balmaseda**, **L. Ferranti**, **F. Vitart**, **F. Molteni**, **F. Doblas-Reyes**, **K. Mogensen** & **A. Vidard**, 2007: Seasonal Forecast System 3. *ECMWF Newsletter No. 110*, 19–5.

Bechtold, **P.**, **M. Köhler**, **T. Jung**, **F. Doblas-Reyes**, **M. Leutbecher**, **M. Rodwell**, **F. Vitart** & **G. Balsamo**, 2008: Advances in simulating atmospheric variability with the ECMWF model: From synoptic to decadal time-scales. *Q. J. R. Meteorol. Soc.*,**134**, 1337–1351.

Jung, **T.**, 2005: Systematic error of the atmospheric circulation in the ECMWF forecasting system. *Q. J. R. Meteorol. Soc.*,**134**, 1337–1351.

McNally, **A.**, **T. Auligné**, **D. Dee** & **G. Kelly**, 2006: A variational approach to satellite bias correction. *ECMWF Newsletter No. 107*, 18–23.

Morcrette, **J.-J.**, **P. Bechtold**, **A. Beljaars**, **A. Benedetti**, **A. Bonet**, **F. Doblas-Reyes**, **J. Hague**, **M. Hamrud**, **J. Haseler**, **J.W. Kaiser**, **M. Leutbecher**, **G. Mozdzynski**, **M. Razinger**, **D. Salmond**, **S. Serrar**, **M. Suttie**, **A. Tompkins**, **A. Untch** & **A. Weisheimer**, 2007: Recent advances in radiation transfer parametrizations. *ECMWF Tech. Memo. No. 539*.

Rodwell, **M.J.** & **B.J. Hoskins**, 1996: Monsoons and the dynamics of deserts. *Q. J. R. Meteorol. Soc.*, **122**, 1385–1404.

Rodwell, **M.J.** & **T. Jung**, 2008: Understanding the local and global impacts of model physics changes: An aerosol example. *Q. J. R. Meteorol. Soc.*, **134**, 1479–1497.

The EU-funded BRIDGE project

BAUDOUIN RAOULT, CRISTIAN CODOREAN

BRIDGE is a project funded by the European Commission under the sixth Framework Programme - Information Society Technologies (FP6-IST). The project started in January 2007 and was scheduled to last for two years. The aim of the project is to demonstrate the benefits of GRID technologies for international co-operation, in particular between Europe and China. The BRIDGE project covers three application areas: pharmaceuticals, aeronautics and meteorology.

The BRIDGE project provides the partners of the meteorological activity with an opportunity to address the development of the next phase of the THORPEX Interactive Grand Global Ensemble programme, otherwise known as TIGGE (see *ECMWF Newsletter No. 116*). In this next phase the data archives are distributed over a number of repositories, instead of all being held centrally (as in the first phase), but efficient and transparent access to users is maintained.

The aim of the meteorological activity in BRIDGE, which involves ECMWF, DWD and the China Meteorological Administration (CMA), is to build an infrastructure to provide distributed access to the TIGGE databases at ECMWF and CMA. This infrastructure will be used to explore ways of creating probabilistic forecast products in a distributed fashion. The main challenge will come from the sheer volume of data involved: methods will have to be found to use the data efficiently with minimal data transfers.

Design and concepts

The aim of the BRIDGE application is to implement distributed processing on distributed data while minimising data transfers. The distributed computational and archiving facilities may reside on different continents. It is expected that:

- Each site will host only part of the data.
- Each site will offer basic data manipulation services (e.g. computing an average).

During the analysis phase of the project, the concepts of '*products*' and '*operations*' were defined. A product (e.g. an ensemble mean) can be defined in terms of basic operations (e.g. data retrievals and averages).

Depending on their nature, some operations can be '*decomposed*' into elementary operations, which can be run independently.

A typical example of an operation that can be decomposed is the computation of an ensemble mean: assuming that ECMWF holds 50 members and CMA 30 members, we could either transfer the 30 fields from CMA to ECMWF and compute the mean of 80 fields there, or the mean could be computed by summing the 50 fields at ECMWF and summing the 30 fields at CMA, then adding the two partial sums and finally dividing the result by 80. In the first case, we would have to transfer 30 fields across the Internet, while in the second case we would have to transfer only one field.

As illustrated in the example above, it is assumed that intermediate results are usually much smaller than the original data. The adopted strategy to minimize data transfers is to:

- Decompose operations into a set of simpler ones.
- Deploy services that can perform these operations at each site, so that the operations are executed at the data location.
- Transfer the data only when necessary, otherwise exchange data references (URLs).

Using the Metview macro language

Most of the derived products generated twice daily at ECMWF from the Ensemble Prediction System, such as probabilities and distributions, are created using the Metview macro language.

Metview is an interactive meteorological application which enables operational and research meteorologists to access, manipulate and visualise meteorological data on UNIX workstations. It is used at ECMWF and many other meteorological centres to create derived products and plots by means of a powerful macro language.

The Metview Macro language provides researchers with an easy, powerful and comprehensive way to manipulate and display meteorological data. It extends the use of Metview into an operational environment as it enables a user to write complex scripts that may be run with any desired periodicity.

The language supports all the usual flow control statements: `if`, `while`, `repeat`, `for`, `...`, it also supports numbers, strings, dates, lists and associative arrays as types. In addition it implements all the mathematical functions such as `sin()` or `exp()`, following the Fortran convention, so a researcher can easily port existing code into the macro language.

As the aim of the BRIDGE meteorological activity is to create such products in a distributed fashion, it seems natural to reuse an existing production system, i.e. express data access using the MARS query language and adapt the Metview macro language so it can invoke operations on the GRID instead of performing them locally. This will then allow us to easily port existing macros in the BRIDGE environment.

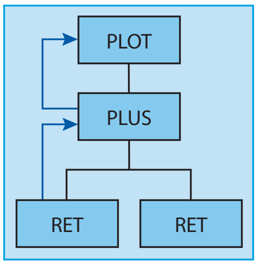

Figure 1 Expression tree.

Implementation

In the context of the BRIDGE project, the Metview language has been extended to support functions which are invocations of GRID services and to support the notion of "remote data". A variable can contain a reference to a piece of data that resides on another site.

The application makes use of the GRIA GRID middleware in Europe and the GOS GRID middleware in China. The interoperability between the two types of middleware is addressed by the project's technology partners.

The main components of the applications are:

- ***script parser*** – parses the Metview scripts.
- ***grid executor*** – maps Metview function calls to GRID service invocations.
- ***cost estimator*** – estimates the cost of invoking a services.

The cost estimator is the central component of the application. Its role is to decide on which site an operation must be performed so that the amount of data transferred is minimal. To illustrate the algorithm, let us consider the following code snippet:

```
plot(retrieve(param:'tp',step:48) +
retrieve(param:'tp',step:24))
```

The script parser will transform it into the expression tree given in Figure 1.

For illustration purposes, it is assumed that one of the retrievals was performed at ECMWF and returned a reference (URL) to a 50 Megabyte file. Similarly, the

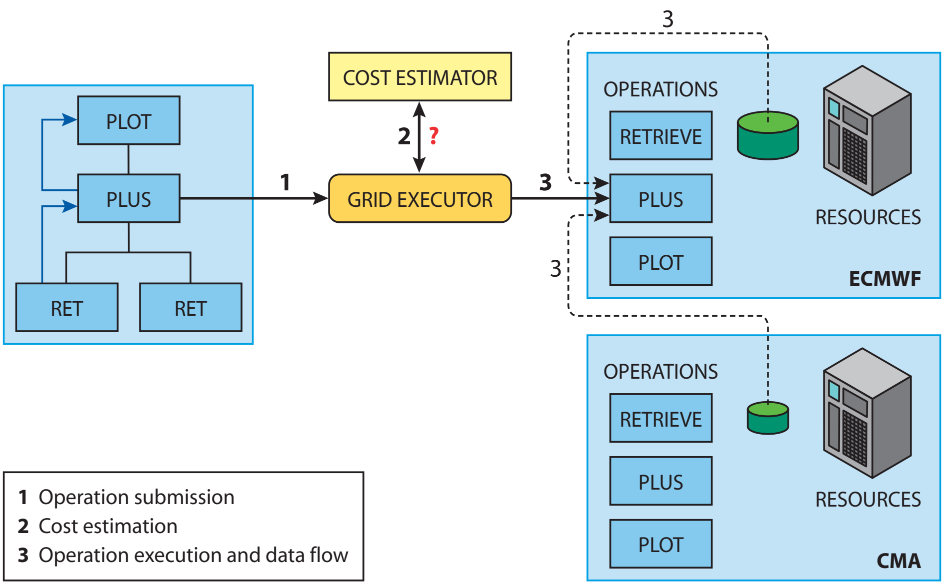

Figure 2 Example of an operation execution.

second retrieval was performed at CMA and returned a URL to a 25 Megabyte file.

The next step is to perform the plus operation. Figure 2 shows how the sequence of calls is carried out.

- The `plus(grib,grib)` operation needs to be dispatched on the GRID. The operation needs to sum two pieces of data, one available at ECMWF and one at CMA (depicted in green in the figure).
- The `plus(grib,grib)` operation is available at both ECMWF and CMA, so we need a way of deciding where to execute the operation.
- The *cost estimator* is the component that will make the decision. The choice is based on selecting the execution scenario with the lowest cost. In the above case, the decision is to dispatch the *plus(grib,grib)* operation at ECMWF because moving the piece of data required by the operation from CMA to ECMWF costs less than moving the data from ECMWF to CMA as the data at CMA is smaller than that at ECMWF.

As we can see from this example, the more sites that offer the same operations, the more possible execution paths there are to choose from. For a medium to long script, the number of choices will grow exponentially with the number of operations performed and the number of services available on the GRID.

The exponential nature of the decision making

a

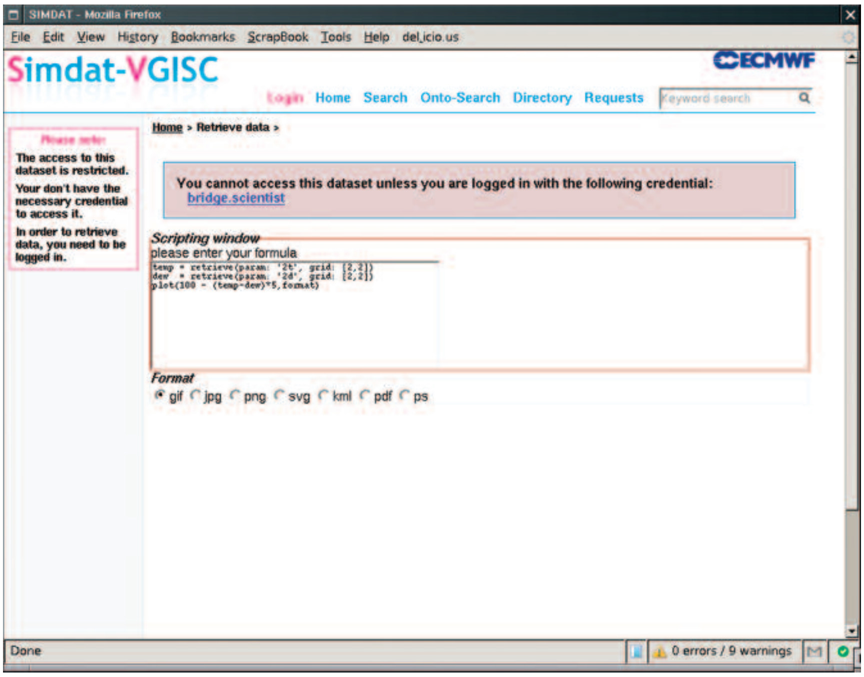

b

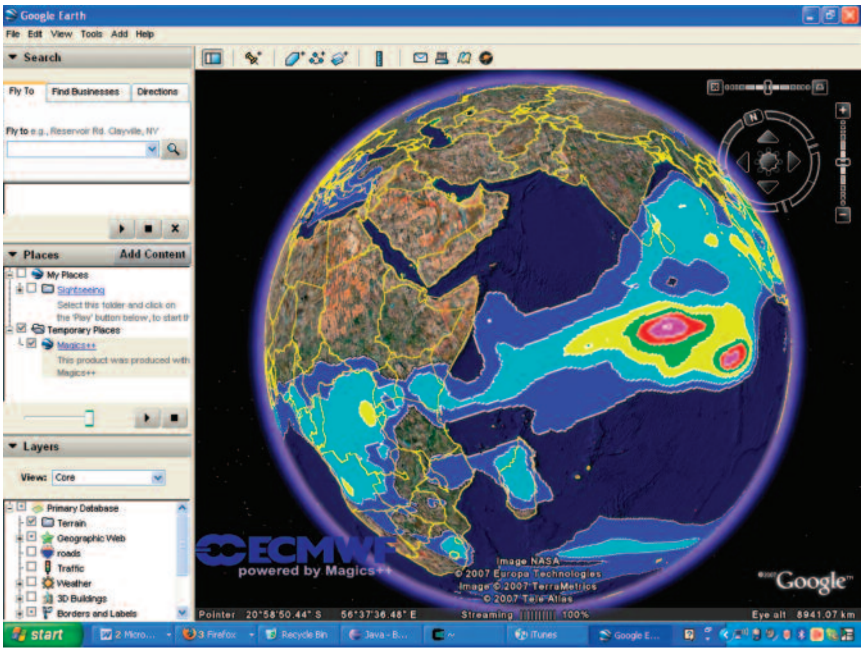

Figure 3 (a) Calculation of the ensemble mean precipitation by accessing BRIDGE from the SIMDAT portal and (b) the result viewed in Google Earth.

prevents any realistic *a priori* evaluation of the cheapest execution path. On the other hand, the chosen solution, where the choices are made dynamically, is scalable and manageable.

Deployment

At this point in the project, the GRID infrastructure has been deployed between ECMWF and CMA, providing access to the TIGGE data held by each site. The GRID has been extended to include services hosted by DWD, with the objective of assessing any DWD-specific requirements and considering their impact on the application prototype, making the system more portable to other sites.

GRID services have been installed at ECMWF, DWD and CMA, using the GRIA and GOS GRID middleware. A Perl package has been written that isolates the implementation of a service from the specific middleware, thus allowing us to deploy the same operations at any of the sites. Currently, the operations that have been deployed provide:

- Access to the TIGGE data from MARS at ECMWF and CMA.
- The creation of plots using Magics^{++}. Some of the following plotting formats are supported: png, gif, jpeg, svg, ps, pdf, kml.
- Manipulation of GRIB data using the grib_api tools.
- All Metview operators and functions on fields (+, /, sin(), cos() sqrt(), stdev(), mean() etc.).
- Csobank: Access to the GME global model from the meteorological database (DWD).
- Climate Data Operators Software (CDO) from the Max-Planck-Institut für Meteorologie for calculations on GRIB fields (DWD).

Deploying the GRID infrastructure has been a challenge, particularly with regard to the security infrastructure of each of the sites.

Integration with SIMDAT

The BRIDGE software has been integrated into the infrastructure of the SIMDAT project. SIMDAT is a four-year EU-funded project aimed at developing generic GRID technology for the solution of complex data-centric problems (see *ECMWF Newsletter No. 104*). A specific data repository has been developed that handles BRIDGE scripts. Consequently a user can now submit, monitor and retrieve the results of scripts submitted through a SIMDAT portal.

Figure 3 shows how to access the ensemble mean precipitation computed with BRIDGE from the SIMDAT portal and the result viewed in Google Earth.

Achievements and provision of further information

The work done as part of the BRIDGE project has demonstrated that the technology exists to perform distributed operations on distributed meteorological data. It has also highlighted some of the difficulties, such as network latency, security and the management of intermediate results.

Several deliverables have been produced that provide detailed information on the architecture and implementation of the BRIDGE software. The source code is available under the Apache 2.0 licence. For more information on the project, please contact the authors at
Baudouin.Raoult@ecmwf.int or
Cristian.Codorean@ecmwf.int.

ECMWF publications

(see http://www.ecmwf.int/publications/)

Technical Memoranda

572 **Engelen, R.J., S. Serrar & F. Chevallier**: Four-dimensional data assimilation of atmospheric CO2 using AIRS observations. *August 2008.*

571 **Benedetti, A., J.-J. Morcrette, O. Boucher, A. Dethof, R.J. Engelen, M. Fisher, H. Flentjes, N. Huneeus, L. Jones, J.W. Kaiser, S. Kinne, A. Mangold, M. Razinger, A.J. Simmons, M. Suttie & GEMS-AER Team**: Aerosol analysis and forecast in the ECMWF Integrated Forecast System: Data assimilation. *August 2008.*

570 **Balmaseda, M.A. & D.L.T. Anderson**: Impact on initialization strategies and observations on seasonal forecast skill. *August 2008.*

569 **Lopez, P.**: Comparison of OPERA precipitation radar composites to CMORPH, SYNOP and ECMWF model data. *August 2008.*

568 **Betts, A.K., M. Köhler & Yuanchong Zhang**: Comparison of river basin hydrometeorology in ERA-Interim and ERA-40 with observations. *July 2008.*

ECMWF Calendar 2009

Feb 2–Mar 6	Training Course – Use of computing facilities
Feb 2–6	*Introduction to HPCF*
Feb 9–11	*GRIB API: library and tools*
Feb 11–13	*Introduction to SMS/XCDP*
Feb 23–27	*Introduction for new users / MARS*
Mar 2–3	*MAGICS*
Mar 4–6	*METVIEW*
Mar 9–13	Training Course – Use and interpretation of ECMWF products
Mar 16–May 21	Training Course – Numerical Weather Prediction
Mar 16–25	*Predictability, diagnostics and seasonal forecasting*
Mar 30–Apr 3	*Numerical methods and adiabatic formulation of models*
Apr 20–29	*Data assimilation and use of satellite data*
May 11–21	*Parametrization of diabatic processes*
Apr 27–28 (tbc)	Advisory Committee on Data Policy (*10th Session*)
Apr 28–29	Finance Committee (*82nd Session*)
Apr 29–30 (tbc)	Policy Advisory Committee (*27th Session*)
May 6–8	Workshop on "Use of IASI Data"
May 11–12	Security Representatives' Meeting
May 12–14	Computer Representatives' Meeting
Jun 1–5	Training Course – Use and interpretation of ECMWF products
Jun 10–12	Forecast Products – Users' Meeting
Jun 15–17	Workshop on "Diagnostics of Data Assimilation System Performance"
Jun 25–26	Council (*71st Session*)
Sep 7–10	Seminar on "Diagnostic Techniques to Understand and Improve Forecasting Systems"
Sep 30–Oct 2	Scientific Advisory Committee (*38th Session*)
Oct 5–7	Technical Advisory Committee (*40th Session*)
Oct 12–16	Training Course – Use and interpretation of ECMWF products for WMO Members
Oct 12–13	Finance Committee (*83rd Session*)
Oct 13–14 (tbc)	Policy Advisory Committee (*28th Session*)
Oct 19 (tbc)	Advisory Committee of Co-operating States (*15th Session*)
Nov 2–6	12th Workshop on "Meteorological Operational Systems"
Nov 9–11	12th Workshop on "Non-hydrostatic Modelling"
Nov 23–26	Workshop on "Monitoring Atmospheric Composition and Climate (MACC)"
Dec 8–9	Council (*72nd Session*)

Index of past newsletter articles

This is a selection of articles published in the ECMWF Newsletter series during the last five years. Articles are arranged in date order within each subject category. Articles can be accessed on the ECMWF public website – www.ecmwf.int/publications/newsletter/index.html

Ensemble prediction and Seasonal Forecasting

	No.	Date	Page
Using the ECMWF reforecast dataset to calibrate EPS forecasts	117	Autumn 2008	8
The THORPEX Interactive Grand Global Ensemble (TIGGE): concept and objectives	116	Summer 2008	9
Implementation of TIGGE Phase 1	116	Summer 2008	10
Predictability studies using TIGGE data	116	Summer 2008	16
Merging VarEPS with the monthly forecasting system: a first step towards seamless prediction	115	Spring 2008	35
Seasonal forecasting of tropical storm frequency	112	Summer 2007	16
New web products for the ECMWF Seasonal Forecast System-3	111	Spring 2007	28
Seasonal Forecast System 3	110	Winter 2006/07	19
The ECMWF Variable Resolution Ensemble Prediction System (VAREPS)	108	Summer 2006	14
Limited area ensemble forecasting in Norway using targeted EPS	107	Spring 2006	23
Ensemble prediction: A pedagogical perspective	106	Winter 2005/06	10
Comparing and combining deterministic and ensemble forecasts: How to predict rainfall occurrence better	106	Winter 2005/06	17
EPS skill improvements between 1994 and 2005	104	Summer 2005	10
Ensembles-based predictions of climate change and their impacts (ENSEMBLES Project)	103	Spring 2005	16
Monthly forecasting	100	Spring 2004	3

Ocean and wave modelling

	No.	Date	Page
Climate variability from the new System 3 ocean reanalysis	113	Autumn 2007	8
Progress in wave forecasts at ECMWF	106	Winter 2005/06	28
Ocean analysis at ECMWF: From real-time ocean initial conditions to historical ocean analysis	105	Autumn 2005	24
High-precision gravimetry and ECMWF forcing for ocean tide models	105	Autumn 2005	6
Towards freak-wave prediction over the global oceans	100	Spring 2004	24

Environmental monitoring

	No.	Date	Page
GEMS aerosol analyses with the ECMWF Integrated Forecast System	116	Summer 2008	20
Progress with the GEMS project	107	Spring 2006	5
A preliminary survey of ERA-40 users developing applications of relevance to GEO (Group on Earth Observations)	104	Summer 2005	5
The GEMS project – making a contribution to the environmental monitoring mission of ECMWF	103	Spring 2005	17

Meteorological applications and studies

	No.	Date	Page
The ECMWF 'Diagnostic Explorer': A web tool to aid forecast system assessment and development	117	Autumn 2008	21
Diagnosing forecast error using relaxation experiments	116	Summer 2008	24
ECMWF's contribution to AMMA	115	Spring 2008	19
Coupled ocean-atmosphere medium-range forecasts: the MERSEA experience	115	Spring 2008	27
Probability forecasts for water levels in The Netherlands	114	Winter 2007/08	23
Impact of airborne Doppler lidar observations on ECMWF forecasts	113	Autumn 2007	28
Ensemble streamflow forecasts over France	111	Spring 2007	21
Hindcasts of historic storms with the DWD models GME, LMQ and LMK using ERA-40 reanalyses	109	Autumn 2006	16
Hurricane Jim over New Caledonia: a remarkable numerical prediction of its genesis and track	109	Autumn 2006	21
Recent developments in extreme weather forecasting	107	Spring 2006	8
MERSEA – a project to develop ocean and marine applications	103	Spring 2005	21
Starting-up medium-range forecasting for New Caledonia in the South-West Pacific Ocean – a not so boring tropical climate	102	Winter 2004/05	2
A snowstorm in North-Western Turkey 12–13 February 2004 – Forecasts, public warnings and lessons learned	102	Winter 2004/05	15
Early medium-range forecasts of tropical cyclones	102	Winter 2004/05	7
European Flood Alert System	101	Sum/Aut 2004	30

Useful names and telephone numbers within ECMWF

Telephone
Telephone number of an individual at the Centre is:

International: +44 118 949 9 + three digit extension
UK: (0118) 949 9 + three digit extension
Internal: 2 + three digit extension

e.g. the Director's number is:
+44 118 949 9001 (international),
(0118) 949 9001 (UK) and 2001 (internal).

E-mail
The e-mail address of an individual at the Centre is:
firstinitial.lastname@ecmwf.int

e.g. the Director's address is: D.Marbouty@ecmwf.int

For double-barrelled names use a hyphen
e.g. J-N.Name-Name@ecmwf.int

Internet web site
ECMWF's public web site is: http://www.ecmwf.int

	Ext
Director	
Dominique Marbouty	001
Deputy Director & Head of Research Department	
Philippe Bougeault	005
Head of Operations Department	
Walter Zwieflhofer	003
Head of Administration Department	
Ute Dahremöller	007

	Ext
Switchboard	
ECMWF switchboard	000
Advisory	
Internet mail addressed to Advisory@ecmwf.int	
Telefax (+44 118 986 9450, marked User Support)	
Computer Division	
Division Head	
Isabella Weger	050
Computer Operations Section Head	
Sylvia Baylis	301
Networking and Computer Security Section Head	
Rémy Giraud	356
Servers and Desktops Section Head	
Richard Fisker	355
Systems Software Section Head	
Neil Storer	353
User Support Section Head	
Umberto Modigliani	382
User Support Staff	
Paul Dando	381
Dominique Lucas	386
Carsten Maaß	389
Pam Prior	384
Computer Operations	
Call Desk	303
Call Desk email: calldesk@ecmwf.int	
Console – Shift Leaders	803
Console fax number +44 118 949 9840	
Console email: newops@ecmwf.int	
Fault reporting – Call Desk	303
Registration – Call Desk	303
Service queries – Call Desk	303
Tape Requests – Tape Librarian	315

	Ext
Meteorological Division	
Division Head	
Erik Andersson	060
Meteorological Applications Section Head	
Alfred Hofstadler	400
Data and Services Section Head	
Baudouin Raoult	404
Graphics Section Head	
Stephan Siemen	375
Meteorological Operations Section Head	
David Richardson	420
Meteorological Analysts	
Antonio Garcia-Mendez	424
Anna Ghelli	425
Claude Gibert (web products)	111
Fernando Prates	421
Meteorological Operations Room	426
Data Division	
Division Head	
Jean-Noël Thépaut	030
Data Assimilation Section Head	
Lars Isaksen	852
Satellite Data Section Head	
Peter Bauer	080
Re-Analysis Section Head	
Dick Dee	352
Probabilistic Forecasting & Diagnostics Division	
Division Head	
Tim Palmer	600
Seasonal Forecasting Section Head	
Franco Molteni	108
Model Division	
Division Head	
Martin Miller	070
Numerical Aspects Section Head	
Agathe Untch	704
Physical Aspects Section Head	
Anton Beljaars	035
Ocean Waves Section Head	
Peter Janssen	116
GMES Coordinator	
Adrian Simmons	700
Education & Training	
Renate Hagedorn	257
ECMWF library & documentation distribution	
Els Kooij-Connally	751